

## A NUMERICAL ALGORITHM FOR SET-POINT REGULATION OF NON-LINEAR PARABOLIC CONTROL SYSTEMS

EUGENIO AULISA AND DAVID GILLIAM

**Abstract.** In this paper we hope to draw attention to a particularly simple and extremely flexible design strategy for solving a wide class of “set-point” regulation problems for nonlinear parabolic boundary control systems. By this we mean that the signals to be tracked and disturbances to be rejected are time independent. The theoretical underpinnings of our approach is the well known regulator equations from the geometric theory of regulation applicable in the neighborhood of an equilibrium. The most important point of this work is the wide applicability of the design methodology. In the examples we have employed unbounded sensing and actuation but the method works equally well for bounded input and output operators and even finite dimensional nonlinear control systems. Our examples include: multi-input multi-output regulation for a boundary controlled viscous Burgers’ equation; control of a Navier-Stokes flow in two dimensional forked channel; control problem for a non-Isothermal Navier-Stokes flow in two dimensional box domain. Along the way we provide some discussion to demonstrate how the method can be altered to provide many alternative control mechanisms. In particular, in the last section we show how the method can be adapted to solve tracking and disturbance rejection for piecewise constant time dependent signals.

**Key words.** Boundary Control System, Center Manifold, Regulator Equations.

### 1. Introduction

In control theory, regulation of a control system is a fundamental problem that has received considerable attention in the engineering literature. Specific examples of regulation problems include the design of control laws that achieve tracking and disturbance rejection. Our interest in this paper is to present a straightforward methodology for numerical implementation of a strategy (based on the geometric theory of regulation) for solving a wide variety of regulation problems for linear and nonlinear distributed parameter systems with quite general control and sensing, including boundary control and sensing. In the geometric theory of regulation, problems of output regulation include asymptotic tracking of reference signals and rejection of unwanted disturbances. This methodology was first studied by B. Francis [8] and many others in the finite dimensional linear case. In a series of tremendously inspiring papers in the early 1990s, C. I. Byrnes and A. Isidori [11, 12, 13] extended the geometric theory to nonlinear finite dimensional systems. Byrnes and Isidori’s work was based on center manifold theory and reduced the design problem to solving a pair of nonlinear operator equations referred to as the Regulator Equations. These equations are also often called the FBI equations after Francis, Byrnes and Isidori. Until recently, a major obstacle to the practical implementation of the method was the inherent difficulty in solving the Regulator Equations. In this area we have made significant progress toward obtaining approximate numerical solutions by developing methods for solving the nonlinear regulator equations. Our techniques have lead to the ability to design control laws even for such complicated systems as the two dimensional Boussinesq approximation of non-isothermal incompressible flows.

---

Received by the editors June 16, 2012 and, in revised form, August 13, 2012.

2000 *Mathematics Subject Classification.* 93C20, 35B37, 93C10, 93B40; 93B52, 93B27, 65N12, 65Y99.

The explicit examples presented in this work (Section 4 and Section 5) are concerned with applications from distributed parameter control in which the plant is given in terms of a nonlinear parabolic partial differential equation. The main reason for our choice of examples is that they provide the most challenging types of examples. In particular, for systems governed by partial differential equations it is not only possible for the state operator to be unbounded but also the input and output maps as well. Here, the expression unbounded means discontinuous. For example, output mappings defined by point evaluation at points or on lower dimensional hypersurfaces either inside the spatial domain or on the boundary of this domain provide discontinuous (unbounded) mappings in the standard  $L^2$  energy Hilbert space. Indeed, in the terminology of functional analysis such operators may not even be closable. Similarly, control inputs that enter through the boundary or inside the spatial domain at points or on lower dimensional hypersurfaces are also described by distributional operators which are unbounded mappings in the standard  $L^2$  Hilbert space.

It would have been easier to include examples with bounded input and output maps and even examples from finite dimensional control theory since the basic methodology described in this work applies equally well to linear or nonlinear regulation control problems for these types of systems. We hope that the interested reader can easily adapt the roadmap presented here to solve problems for other types of set point control problems.

As we have already mentioned this paper is concerned with set-point regulation problems. These are problems in which the reference signals to be tracked and disturbances to be rejected are independent of time. We focus on this particular class of problems since our numerical algorithm for solving the regulator equations in this case requires a considerably different and much simpler approach than is needed in the more general case of tracking and rejecting time varying signals. The more general case will be the subject of a forthcoming paper [1].

As a disclaimer, in this work we do not investigate the main mathematical properties of the pde models appearing in our application examples. In our opinion such a diversion would seriously detract from the main point of the work which is to exhibit the utility of the design methodology and its numerical implementation. So, for example, we do not go into any details concerning such things as Hilbert space formulations of weak solutions, Sobolev spaces and elliptic estimates needed to guarantee existence and regularity of solutions. To do so would require us to significantly limit the number of examples presented and is not the main point in the work.

The paper is organized as follows. In Section 2 we present the necessary notation and definitions for the general abstract control problem. We briefly discuss the issues related to bounded and unbounded formulations (i.e., boundary type control) and remark that their equivalence have been examined in works such as [15, 16]. In Section 3 we describe the main problem of interest in this work, Problem 3.1. This subsection also contains the details of the design strategy, which derive from the geometric theory of regulation. Our main assumptions, based on the geometric theory of regulation, are captured in Assumptions 3.1 and 3.2. Providing these assumptions are satisfied for a particular control model, it is clear that Problem 3.1 is solvable (at least locally). Section 4 begins with what we consider the most important part of this work, the numerical examples that exhibit the utility of the design strategy presented in Section 3. In Section 5 we provide a general method for tracking and rejecting piecewise constant time dependent signals. The method is

based on the ideas developed in Section 3. We reiterate that this paper is primarily concerned with tracking and disturbance rejection for time independent reference signal. The examples given in Section 5 are intended to show that it is possible to adapt the set-point methodology to handle this slightly more complicated situation. Here we note that the the most important change is prompted by the fact that the controls  $u_j$  described in Problem 3.1 now must be time dependent and therefore the steady state system (21)-(22) must now be replaced by the time dependent system. The resulting system is a DAE that requires regularization. The particular regularization employed is necessary in solving the system (152)-(154), Eq. (156), and the coupling condition (160). In particular for our example it was found that multiplying the time derivative term in Eq. (156) by 0.95 produces a system that is numerically stable. For general time dependent reference and disturbance signals some type of numerical regularization is required. The algorithm and technical details are somewhat more involved and dramatically different from the set point case. As we have already mentioned the general time dependent case will be the subject of a separate paper.

Although all examples have been solved numerically using the finite element software Comsol, for each problem we provide a detailed description of the algorithm, so that its numerical solution can be found by using any alternative PDE package solver. Our choice of using Comsol is motivated by its flexibility for solving coupled multi-physics problems.

## 2. Regulation of Nonlinear Parabolic Control Systems

In this work we are primarily interested in tracking and disturbance rejection for nonlinear parabolic control systems in the form

$$(1) \quad z_t(x, t) = Az(x, t) + F(z(x, t)) + \sum_{j=1}^{n_d} (B_{d_j} d_j)(x, t) + \sum_{j=1}^{n_{in}} (B_{in_j} u_j)(x, t),$$

$$(2) \quad z(x, 0) = z_0(x), \quad z_0 \in \mathcal{Z} = L^2(\Omega),$$

$$(3) \quad y_i(t) = (C_i z)(x, t), \quad i = 1, \dots, n_c,$$

with  $x \in \Omega$ , an open bounded subset of  $\mathbb{R}^n$  with piecewise  $C^2$  boundary, and  $t \geq 0$ . Here  $z(x, t)$  is the state variable and it can be either a scalar or a vector. The terms

$$(4) \quad (B_{d_j} d_j)(x, t) = \Theta_j(x) d_j(t), \quad j = 1, \dots, n_d,$$

$$(5) \quad (B_{in_j} u_j)(x, t) = \Phi_j(x) u_j(t), \quad j = 1, \dots, n_{in},$$

represent disturbances and control inputs, respectively. Note that in Eqs. (4)-(5) each term is a multiplicative operator between a space dependent function and the corresponding input function which is considered to be time dependent only. The expressions  $\Theta_j(x)$  and  $\Phi_j(x)$  are assumed to be known functions, and may also be unbounded (e.g., for example, in the case of boundary control they typically are given by delta functions supported on a portion of the boundary). In general  $B_{d_j}$  refers to a *disturbance input* operator and  $B_{in_j}$  refers to a *control input* operator.

In this paper the state operator  $A$  is assumed to be a linear differential operator in an infinite dimensional Hilbert state space  $\mathcal{Z} = L^2(\Omega)$ . It is assumed that the operator  $A$  defined on a dense domain  $\mathcal{D}(A)$  generates an exponentially stable  $C_0$  semigroup in  $\mathcal{Z}$ . In our intended applications the operators  $C_i$  in Eq. (3) are typically point evaluation or a weighted integral of the solution  $z(x, t)$  in some part of the domain  $\Omega$  or its boundary. Therefore these operators are generally densely

defined and not usually bounded in the the state space  $\mathcal{Z}$ . The most common situation is that  $-A$  is an accretive operator that generates a Hilbert scale of spaces  $\mathcal{Z}_\alpha$  for  $\alpha \in \mathbb{R}$  and the domain of  $C_i$ , denoted by  $\mathcal{D}(C_i)$ , is contained in some  $\mathcal{Z}_{\alpha_0}$  for some  $\alpha_0 > 0$ . So we assume that  $C_i : \mathcal{D}(C_i) \rightarrow \mathbb{R}$  for each  $i$  (see, e.g., [10, 14]).

We assume that the boundary of  $\Omega$ , denoted by  $\partial\Omega$ , is piecewise  $C^2$  and is represented by the union of  $(n - 1)$  dimensional connected hypersurfaces  $\mathcal{S}_j$ , which are subsets of  $\partial\Omega$  and whose interiors are pairwise disjoint.

Here the nonlinear function  $F$  is a smooth function with  $F(0) = 0$  so that the uncontrolled plant has the origin in  $\mathcal{Z}$  as an exponentially stable equilibrium.

**Remark 2.1.** Stability of the the origin for the uncontrolled nonlinear problem, i.e., the problem with all  $u_j = 0$  and  $d_j = 0$ , is a critical component of the theoretical development (see [12, 13, 4]) of the geometric approach to regulation based on center manifold theory. Here by stability we mean that for all sufficiently small initial data  $z_0 \in \mathcal{Z}$ , say  $\|z_0\| \leq \delta$ , there exists positive constants  $M$  and  $\alpha$  (depending on  $\delta$ ) so the solution of

$$\begin{aligned} z_t(x, t) &= Az(x, t) + F(z(x, t)), \\ z(x, 0) &= z_0(x), \end{aligned}$$

satisfies

$$\|z(\cdot, t)\| \leq Me^{-\alpha t} \quad \text{for all } t \geq 0.$$

If the operator  $A$  is not stable, (does not generate a stable semigroup) then we must first introduce a feedback mechanism that stabilizes the plant. The problem of finding such a feedback law is the stabilization problem and is not the same as the regulator problem considered here. Since our interest is with tracking and disturbance rejection and not stabilization we assume that the plant in question is already stable in order to avoid the extra layer of complication.

**2.1. Standard Control Systems Form.** The vast majority of the distributed parameter control results are stated in what is often referred to as standard system form. Introducing a few new notations allows us to write the control system (1)-(3) in the standard system theoretic state space form. Namely, let us define

$$(6) \quad D = \begin{bmatrix} d_1 \\ d_2 \\ \vdots \\ d_{n_d} \end{bmatrix}, \quad U = \begin{bmatrix} u_1 \\ u_2 \\ \vdots \\ u_{n_{in}} \end{bmatrix}, \quad Y = \begin{bmatrix} y_1 \\ y_2 \\ \vdots \\ y_{n_c} \end{bmatrix}, \quad Y_r = \begin{bmatrix} y_{r,1} \\ y_{r,2} \\ \vdots \\ y_{r,n_c} \end{bmatrix}.$$

With this notation we can write our control problem as

$$(7) \quad \frac{dz}{dt} = Az + F(z) + B_d D + B_{in} U,$$

$$(8) \quad Y = Cz.$$

Here we have written the input, disturbance and output terms in matrix form as

$$B_d D = \sum_{j=1}^{n_d} \Theta_j(x) d_j(t), \quad B_{in} U = \sum_{j=1}^{n_{in}} \Phi_j(x) u_j(t), \quad Y = Cz = \begin{bmatrix} C_1(z) \\ C_2(z) \\ \vdots \\ C_{n_c}(z) \end{bmatrix},$$

where  $B_d$  and  $B_{in}$  are disturbance input and control input operators respectively, and  $C$  denotes the output operator.

**2.2. Formulation for Boundary Control Systems.** In situations involving distributed parameter systems governed by partial differential equations it very often happens that the control inputs and the disturbances influence the system through the boundary.

In the several explicit examples presented in this paper some of the operators  $B_{\text{in},j}$  and  $B_{\text{d},j}$  in the system (1)-(3) correspond to boundary control operators. That is to say they correspond to controls or disturbances that enter through boundary conditions on the hypersurfaces  $\mathcal{S}_j$  or at points or on hypersurfaces inside the domain. In system (1)-(3) the boundary conditions are included in the input operators  $B_{\text{d},j}$  and  $B_{\text{in},j}$ , for some set of indices. Let the sequences  $B_{\text{d},j}$  and  $B_{\text{in},j}$  be ordered so that the first  $n_{\text{d}}^b$  and  $n_{\text{in}}^b$  elements correspond to boundary operators  $\mathcal{B}_{\text{d},j}$  and  $\mathcal{B}_{\text{in},j}$  defined on the hypersurfaces  $\mathcal{S}_{\text{d},j}$  and  $\mathcal{S}_{\text{in},j}$  respectively. Then the control system (1) can be written in the equivalent form

$$(9) \quad z_t(x, t) = A_0 z(x, t) + F(z(x, t)) + \sum_{j=n_{\text{d}}^b+1}^{n_{\text{d}}} (B_{\text{d},j} d_j)(x, t) \\ + \sum_{j=n_{\text{in}}^b+1}^{n_{\text{in}}} (B_{\text{in},j} u_j)(x, t),$$

$$(10) \quad (\mathcal{B}_{\text{d},j} z)(x, t) = \vartheta_j(x) d_j(t), \quad x \in \mathcal{S}_{\text{d},j}, \quad j = 1, \dots, n_{\text{d}}^b,$$

$$(11) \quad (\mathcal{B}_{\text{in},j} z)(x, t) = \varphi_j(x) u_j(t), \quad x \in \mathcal{S}_{\text{in},j}, \quad j = 1, \dots, n_{\text{in}}^b.$$

where  $z = z(x, t)$ , (10), (11) are boundary disturbance and control input terms which replace the homogeneous boundary conditions which are hidden in the definition of  $\mathcal{D}(A)$ .

We note that in this case the functions  $\vartheta_j(x)$  in (10) and  $\varphi_j(x)$  in (11) are not the same as the distributional functions  $\Theta_j$  and  $\Phi_j$  given in (4) and (5). Indeed, the functions  $\vartheta_j(x)$  and  $\varphi_j(x)$  are typically smooth functions, not distributions. The reformulation of problem (1)-(5) into the form (9)-(11) is discussed in [2, 15, 16]. In particular, it is well known that under suitable assumptions there exist operators  $B_{\text{d},j}$  and  $B_{\text{in},j}$  so that system (9)-(11) can be written in the form (1) (cf. [2, 15, 16]). Here the operator  $A_0$  is typically a linear elliptic partial differential operator engendered with only a partial set of boundary conditions. We denote the dense domain of  $A_0$  in  $\mathcal{Z}$  by  $\mathcal{D}(A_0)$ .

The operator  $A$  is the same linear elliptic partial differential operator  $A_0$  with domain, denoted by  $\mathcal{D}(A)$ , given by

$$(12) \quad \mathcal{D}(A) = \{\varphi : \mathcal{B}_{\text{d},j} \varphi = 0 \ (j = 1, \dots, n_{\text{d}}^b), \ \mathcal{B}_{\text{in},j} \varphi = 0 \ (j = 1, \dots, n_{\text{in}}^b)\} \cap \mathcal{D}(A_0).$$

The structure of the boundary operators depends on the structure of the operator  $A$  and other physical properties of the particular problem. Generally speaking the boundary operators  $\mathcal{B}_{\text{d},j}$  and  $\mathcal{B}_{\text{in},j}$  can represent any of the classical boundary conditions, including Dirichlet, Neumann and Robin, etc. The explicit examples in this work provide a clear description of the general types of boundary conditions that can be handled with this methodology.

As a simple example, consider a control system modeled by a one dimensional heat equation on a unit interval, e.g.,  $0 < x < 1$ . With temperature at  $x$  at time  $t$  denoted by  $z(x, t)$ , suppose that the left end of the rod is held at a constant temperature  $d$  (a constant disturbance) and we are able to control the flow of heat into or out of the the rod at the right end of the rod (a flux boundary control). This system, with initial temperature distribution  $z_0(x)$  would normally be written

as an initial boundary value problem in the Hilbert state space  $\mathcal{Z} = L^2(0, 1)$  as

$$(13) \quad z_t(x, t) = z_{xx}(x, t),$$

$$(14) \quad z(0, t) = d,$$

$$(15) \quad z_x(1, t) = u,$$

$$(16) \quad z(x, 0) = z_0(x).$$

An example of a set point control problem would be to find a control  $u$  in order to drive the temperature at a given point,  $0 < x_0 < 1$ , to a constant value  $M$ . In this case our measured output would be  $z(x_0, t)$  and our reference signal would be  $y_r = M$ . The “boundary control” system (13)-(16) can be transformed in an equivalent form as the system

$$(17) \quad z_t(x, t) = Az(x, t) + \frac{d\delta_0}{dx}d + \delta_1u,$$

$$(18) \quad z(x, 0) = z_0(x),$$

where  $\delta_j$  for  $j = 0, 1$  denote the Dirac delta function supported at  $x = 0$  and  $x = 1$  respectively. In this form the system now looks like a system written in standard system form as (7)-(8), where

$$B_d = \frac{d\delta_0}{dx} \text{ and } B_{in} = \delta_1,$$

and

$$A = \frac{d^2}{dx^2} \text{ with domain } \mathcal{D} = \{\varphi \in H^2(0, 1) : \varphi(0) = 0, \varphi'(1) = 0\}.$$

The mathematical problem (17), (18), must be studied in a space of distributions rather than the more desirable space  $L^2(0, 1)$ .

### 3. The Set-Point Control Problem

In this part of the paper we discuss a general strategy intended to deliver control laws capable of solving a wide variety of set point regulation problems, i.e., tracking/disturbance rejection problems for time *independent* reference signals  $y_{r_i} \in \mathbb{R}$ ,  $i = 1, \dots, n_c$ , and disturbances,  $d_j(t) = d_j \in \mathbb{R}$ ,  $i = j, \dots, n_d$ . In Section 5 we discuss a methodology for solving tracking and disturbance rejection problems for signals that are time dependent but *piecewise constant* over specified time intervals. We show that for these very special time dependent signals the corresponding tracking problems can be solved with a slight modification of the results of this section. As we have already mentioned, for more general time dependent reference signals and disturbances we refer the reader to a forthcoming paper on the general time dependent case [1].

**Problem 3.1.** *Our design objective is to find a set of time independent controls  $u_j(t) = \gamma_j$ ,  $j = 1, \dots, n_{in}$ , for the system (1)-(3) so that the error defined by*

$$(19) \quad e(t) = \|Y(t) - Y_r\|_\infty = \sup_{1 \leq i \leq n_c} |y_i(t) - y_{r_i}|,$$

*satisfies*

$$(20) \quad e(t) \xrightarrow{t \rightarrow \infty} 0.$$

*while the state of the closed loop plant remains bounded for all time.*

The methodology for solving Problem 3.1 is based on two main assumptions:

**Assumption 3.1.** *There exist constants  $\gamma_j$ ,  $j = 1, \dots, n_{in}$ , and a classical solution  $\bar{z}(x) \in \mathcal{Z}$  of the non-linear elliptic boundary value problem (21) satisfying the constraints given in (22) :*

$$(21) \quad 0 = A\bar{z}(x) + F(\bar{z}(x)) + \sum_{j=0}^{n_d} \theta_j(x)d_j + \sum_{j=0}^{n_{in}} \phi_j(x)\gamma_j,$$

$$(22) \quad C_i\bar{z} = y_{r_i}, \quad i = 1, \dots, n_c.$$

**Assumption 3.2.** *For sufficiently close initial data*

$$\|z_0(x) - \bar{z}(x)\| < \delta,$$

*the solution  $z(x, t)$  of the system (1)-(3) with controls  $u_j = \gamma_j$ , i.e.,*

$$(23) \quad z_t(x, t) = Az(x, t) + F(z(x, t)) + \sum_{j=0}^{n_d} \theta_j(x)d_j + \sum_{j=0}^{n_{in}} \phi_j(x)\gamma_j,$$

$$(24) \quad z(x, 0) = z_0(x),$$

*satisfies*

$$(25) \quad \lim_{t \rightarrow \infty} |C_i z(\cdot, t) - C_i \bar{z}(\cdot)| = 0, \quad i = 1, \dots, n_{in}.$$

Clearly the condition in (25) implies the asymptotic error condition (20), i.e., under Assumptions 3.1 and 3.2, it is obvious that

$$y_i(t) = C_i z \xrightarrow{t \rightarrow \infty} C_i \bar{z} = y_{r_i}, \quad i = 1, \dots, n_{in}.$$

Thus the solution of our set-point control problem is  $u_j = \gamma_j$ ,  $j = 1, \dots, n_{in}$ , which is obtained, along with  $\bar{z}$ , by solving the system (21)-(22).

**Remark 3.1.** The output operators  $C_i$  are often given as point evaluation or as the weighted average of the state  $z(x, t)$  on a hypersurface  $\mathcal{S}_i$  inside or on the boundary of  $\Omega$ , i.e.,

$$(26) \quad y_i(t) = C_i z = \frac{1}{|\mathcal{S}_i|} \int_{\mathcal{S}_i} z(x, t) d\sigma_x,$$

where by  $d\sigma_x$  we denote the natural hypersurface measure on  $\mathcal{S}_i$ . For example it could be that  $\mathcal{S}_i$  is one of the boundary patches  $\mathcal{S}_j$ . We note that the operators  $C_i$  are well defined in our setting since in a typical parabolic problem the state  $z(\cdot, t)$  for  $t > 0$  is contained in  $C^\infty(\bar{\Omega})$  so that the trace on the boundary of  $\Omega$  is a continuous function.

Assumptions 3.1 and 3.2 are motivated by the development of C.I. Byrnes and A. Isidori [11, 12, 13] for finite dimensional nonlinear equations. Their approach is based on invariant manifold theory in a neighborhood of an equilibrium, and requires solving a pair of operator equations referred to as the regulator equations. It is further assumed that the disturbances  $d_j(t)$  and signals to be tracked  $y_{r_i}(t)$  are generated as outputs of a neutrally stable, finite dimensional exogenous system. The case of set point control, where all the  $d_j$  and  $y_{r_i}$  are time independent, satisfies this requirement. In particular the exo-system in this case is given by

$$(27) \quad \frac{dw}{dt} = Sw, \quad w(0) = w_0,$$

where  $w = [w_1, w_2, \dots, w_{n_c+n_d}]^\top \in \mathcal{W} = \mathbb{R}^{n_c+n_d}$ ,  $S$  is the  $(n_c + n_d) \times (n_c + n_d)$  zero matrix, and

$$(28) \quad w_0 = [y_{r_1}, \dots, y_{r_{n_c}}, d_1, \dots, d_{n_d}]^\top.$$

Clearly the solution to the initial value problem (27) is the constant vector  $w(t) = w_0$  for all times.

In the geometric theory we seek controls  $u_j$  as a feedback of the state of the exo-system, i.e.,  $u_j = \gamma_j(w)$ , which we will often denote simply by  $\gamma_j$ . So in particular in this case we seek controls that are time independent. In matrix form we have

$$U = \begin{bmatrix} u_1 \\ \vdots \\ u_{n_{\text{in}}} \end{bmatrix} = \begin{bmatrix} \gamma_1 \\ \vdots \\ \gamma_{n_{\text{in}}} \end{bmatrix}.$$

By assumption  $A$  is the generator of an exponentially stable semigroup and therefore its spectrum lies in the strict left half complex plane.

In this case the closed loop system, consisting of (1)-(3) coupled with (27) and controls  $u_j = \gamma_j(w)$ , is given in the state space  $\mathcal{Z} \times \mathcal{W}$  as

$$(29) \quad z_t = Az + F(z) + \sum_{j=0}^{n_d} B_{d_j} d_j(w) + \sum_{j=0}^{n_{\text{in}}} B_{\text{in}_j} \gamma_j(w),$$

$$(30) \quad \frac{dw}{dt} = Sw,$$

$$(31) \quad z(x, 0) = \varphi(x), \quad w(0) = w_0.$$

The linearization of this problem has spectrum consisting of the spectrum of  $A$  together with the spectrum of  $S$ . So there are  $n_d + n_c$  eigenvalues at zero (on the imaginary axis) and the remainder of the spectrum is in the left half complex plane. In the terminology of dynamical systems, the problem has an infinite dimensional stable manifold and a  $n_d + n_c$  dimensional center manifold. Further, solutions beginning in a sufficiently small neighborhood of the origin in  $\mathcal{Z} \times \mathcal{W}$  converge exponentially to a solution on the  $n_d + n_c$  dimensional center manifold. In the set point case this solution is a point on the center manifold corresponding to the single point  $w_0$ .

In order to obtain the controls  $\gamma_j$ , C.I. Byrnes and A. Isidori [11, 12, 13] approach involves finding a so-called error zeroing center manifold. In the mathematical terminology of invariant manifolds we seek an invariant manifold for the dynamics of the closed loop system on which the error, defined in (20), is identically zero. We note that it is possible that such an invariant manifold may not exist. But if it does then we can solve the corresponding regulator problem as follows. We seek a mapping  $\bar{z}(w) : \mathcal{W} \rightarrow \mathcal{Z}$  that expresses the invariance of the  $z$  dynamics of the closed loop system. At least locally, i.e., in a neighborhood  $W_0$  of the origin in  $\mathcal{W}$ , the center manifold  $\Sigma$  is given as the graph of a function in  $\mathcal{Z} \times \mathcal{W}$  space, i.e.,

$$\Sigma = \left\{ \begin{pmatrix} \bar{z}(w) \\ w \end{pmatrix} : w \in W_0 \right\},$$

for some neighborhood  $W_0$  of the origin in  $\mathbb{R}^3$ .

First we note that, by the chain rule, (30), and since  $S = 0$ ,

$$\bar{z}_t = \frac{\partial \bar{z}}{\partial w} w_t = 0.$$

So we obtain from (29)

$$(32) \quad 0 = A\bar{z}(w) + F(\bar{z}(w)) + \sum_{j=0}^{n_d} B_{d_j} d_j(w) + \sum_{j=0}^{n_{\text{in}}} B_{\text{in}_j} \gamma_j(w),$$

which is precisely (21). The requirement that the invariant manifold be error zeroing means, in addition, that  $\bar{z}$  must satisfy

$$(33) \quad C_i \bar{z}(w) - w_i = 0, \quad i = 1, \dots, n_c,$$

for all  $w$  in a neighborhood of the origin. Recall that by our choice of initial conditions in (28), we have  $w_i = y_{r_i}$ . We conclude that equations (32) and (33) are precisely equations (21), (22) and we see that the Assumptions 3.1 and 3.2 are simply the requirements of the existence of an error zeroing attractive invariant manifold.

**3.0.1. Solution Strategy.** To determine the  $\gamma_j$  that satisfy (21)-(22) we proceed in the following way. First we solve the  $n_{\text{in}}$  linear boundary value problems given by

$$(34) \quad 0 = AX_j(x) + \Phi_j(x), \quad j = 1, \dots, n_{\text{in}} \quad \text{and } x \in \Omega.$$

Notice that as long as the coefficients in these elliptic boundary value problems are sufficiently smooth the solution  $X_j$  will also be smooth by elliptic regularity so that  $X_i \in \mathcal{D}(C_j)$ .

With this we can assemble the matrix  $G_{n_c \times n_{\text{in}}}$ , whose entries are

$$(35) \quad g_{ij} = C_i X_j, \quad i = 1, \dots, n_c, \quad j = 1, \dots, n_{\text{in}}.$$

Each component  $X_j$  belongs to  $\mathcal{Z}$ , and it is the response of the linear operator  $A$  to the input  $\Phi_j$ , namely

$$(36) \quad X_j = -A^{-1}\Phi_j.$$

We rewrite Eq. (21) as

$$(37) \quad \bar{z}(x) = -A^{-1} \left( F(\bar{z}(x)) + \sum_{j=0}^{n_d} \Theta_j(x) d_j \right) + \sum_{j=0}^{n_{\text{in}}} (-A^{-1}\Phi_j(x) \gamma_j),$$

and let  $\tilde{z}(x)$  be the solution of

$$(38) \quad 0 = A\tilde{z} + F(\bar{z}(x)) + \sum_{j=0}^{n_d} \theta_j(x) d_j.$$

Here,  $\tilde{z}$  is the response of the linear operator  $A$  to the sum of the nonlinear term  $F(\bar{z}(x))$  and all the disturbances  $\Theta_j$ , namely

$$(39) \quad \tilde{z} = -A^{-1} \left( F(\bar{z}) + \sum_{j=0}^{n_d} \theta_j(x) d_j \right).$$

Substituting Eqs. (36) and (39) in Eq. (37) yields

$$(40) \quad \bar{z} = \tilde{z} + \sum_{j=0}^{n_{\text{in}}} X_j \gamma_j.$$

Applying the operator  $C_i$  to each side of the above equation, and substituting Eqs. (22) and (35) it follows that

$$(41) \quad y_{r_i} = C_i \bar{z} = C_i \tilde{z} + \sum_{j=0}^{n_{\text{in}}} g_{ij} \gamma_j, \quad i = 1, \dots, n_c.$$

These equations can be written in matrix form as

$$(42) \quad G\Gamma = Y_r - \tilde{Y},$$

where

$$\Gamma = [\gamma_1, \gamma_2, \dots, \gamma_{n_{in}}]^\top, \quad Y_r = [y_{r_1}, y_{r_2}, \dots, y_{r_{n_c}}]^\top, \quad \tilde{Y} = [C_1 \tilde{z}, C_2 \tilde{z}, \dots, C_{n_c} \tilde{z}]^\top.$$

The matrix  $G$  is, in general, a rectangular matrix, and we choose  $\Gamma$  to be the minimal solution of Eq. (42). Because of Assumption 3.1, system (42) is always consistent, and the minimal solution is either the unique solution or, in case of multiple solutions, the solution having the least Euclidean norm.

Each equation in (34) is decoupled from the others, thus can be solved individually. In contrast, Eqs. (21), (38) and (42) are fully coupled and should be solved together.

#### 4. Numerical Examples

In this section we present several prototypical examples of tracking and disturbance rejection for nonlinear parabolic boundary control systems. We have chosen more complicated boundary control systems to emphasize how easily these more challenging problems can be handled. Certainly the methodology described in Section 3 can be applied to linear or nonlinear problems with bounded or unbounded observation, actuation and forcing.

**4.1. Burgers' Equation.** In our first example we consider a boundary controlled viscous Burgers' equation

$$(43) \quad z_t(x, t) = \nu z_{xx}(x, t) - z(x, t)z_x(x, t), \quad 0 \leq x \leq 1,$$

with initial condition

$$(44) \quad z(x, 0) = \varphi(x).$$

Here  $\nu$  is a kinematic viscosity and is considered constant on the interval.

The equation (43) is supplemented with a non-homogeneous constant Dirichlet boundary condition at  $x = 0$ ,

$$(45) \quad z(0, t) = d,$$

which we treat as a disturbance.

In addition we have a pair of measured outputs given by point evaluation at the points  $x = 0.25$  and  $x = 0.75$ , respectively

$$(46) \quad y_1(t) = C_1(z) = z(0.25, t),$$

$$(47) \quad y_2(t) = C_2(z) = z(0.75, t).$$

And, finally, we are given a pair of constant reference signals  $y_{r_1}, y_{r_2} \in \mathbb{R}$  to be tracked.

Our objective is to find two constant control inputs  $u_j = \gamma_j$  with  $j = 1, 2$  so that the measured outputs  $y_j$  track the reference signals  $y_{r_j}$  while rejecting the disturbance  $d$ . The first control  $u_1$  enters as a point source in the domain at the point  $x = 0.5$ , and the second control  $u_2$  enters through a Neumann boundary condition at the right end of the interval. In particular we have the following conditions

$$(48) \quad [z(x, t)]_{x=0.5} = 0,$$

$$(49) \quad [\nu z_x(x, t)]_{x=0.5} = u_1,$$

$$(50) \quad \nu z_x(1, t) = u_2,$$

where the notation  $[\varphi]_{x=x_0}$  denotes the jump at  $x_0$  defined by

$$[\varphi]_{x=x_0} = \varphi(x_0^+) - \varphi(x_0^-).$$

Here we have used the notation  $x_0^\pm$  for the limit from the right (+) and the limit from the left (-) at  $x_0$ .

The above description of the problem is illustrated in the Figure 1.

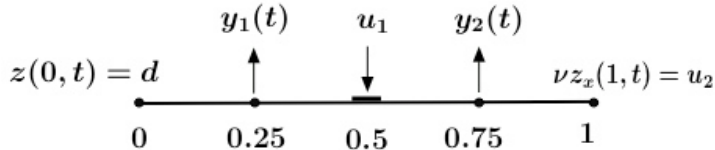


FIGURE 1. Burgers' example domain.

Let us define  $A_0 = \nu d^2/dx^2$  in  $L^2(0, 1)$  with domain  $\mathcal{D}(A_0) = H^2(0, 1)$ . With this, the problem formulated as in Eqs. (9)-(11) can be written using the boundary operators

$$(51) \quad \mathcal{B}_{d_1} z = z(0, t) = d,$$

$$(52) \quad \mathcal{B}_{in_1} z = \begin{cases} [z(x, t)]_{x=0.5} = 0 \\ [\nu z_x(x, t)]_{x=0.5} = u_1 \end{cases},$$

$$(53) \quad \mathcal{B}_{in_2} z = \nu z_x(1, t) = u_2.$$

The same problem can be formulated in state space form as in Eqs. (1)-(3) by introducing the equivalent distributional terms

$$(54) \quad B_{d_1} d = \frac{d\delta_0}{dx} d,$$

$$(55) \quad B_{in_1} u_1 = -\delta_{0.5} u_1,$$

$$(56) \quad B_{in_2} u_2 = \delta_1 u_2,$$

where  $\delta_{x_0}$  is the Dirac delta distribution supported at  $x = x_0$ .

For this example the nonlinear term in (1) is  $F(z) = -z z_x$ .

**Remark 4.1.** It should be noticed that the boundary operators in (51) and (53) produce the classical Dirichlet and Neumann boundary conditions, and the operator (51) imposes a jump in the first derivative of the solution. The operators (54)-(56) are their equivalent distributional counterpart. When solving a partial differential equation with finite element methods it is generally easier to deal with the Dirichlet boundary operator (51) rather than (54); in case of Neumann boundary conditions (53) and (56) result in the same forcing term; to force the jump in the solution first derivative it is straightforward to use (55) rather than (52). In the rest of the paper we will consider the operators that are more convenient, keeping in mind that there always exist these alternative counterparts.

From here the problem is solved numerically by proceeding exactly as described in the Section 3. First we must solve for  $X_j$ ,  $j = 1, 2$ , but rather than solving the equations as written in (34) we solve

$$(57) \quad \nu \frac{d^2 X_1}{dx^2} = \delta_{0.5}, \quad \text{for } 0 < x < 1$$

$$(58) \quad X_1(0) = 0, \quad \nu \frac{dX_1}{dx}(1) = 0,$$

for  $X_1$ , and

$$(59) \quad \nu \frac{d^2 X_2}{dx^2} = 0, \quad \text{for } 0 < x < 1,$$

$$(60) \quad X_2(0) = 0, \quad \nu \frac{dX_2}{dx}(1) = 1,$$

for  $X_2$ . These still produce the desired functions

$$(61) \quad X_1 = (-A)^{-1}B_{in1} \quad \text{and} \quad X_2 = (-A)^{-1}B_{in2},$$

and the entries of the  $2 \times 2$  matrix

$$(62) \quad G = \begin{pmatrix} C_1 X_1 & C_1 X_2 \\ C_2 X_1 & C_2 X_2 \end{pmatrix}.$$

With this, we now solve the steady state coupled system

$$(63) \quad 0 = \nu \frac{d^2 \bar{z}}{dx^2} - \bar{z} \frac{d\bar{z}}{dx} - \delta_{0.5} \gamma_1, \quad \text{for } 0 < x < 1,$$

$$(64) \quad \bar{z}(0) = d, \quad \nu \frac{d\bar{z}}{dx}(1) = \gamma_2,$$

$$(65) \quad 0 = \nu \frac{d^2 \tilde{z}}{dx^2} - \tilde{z} \frac{d\tilde{z}}{dx}, \quad \text{for } 0 < x < 1,$$

$$(66) \quad \tilde{z}(0) = d, \quad \nu \frac{d\tilde{z}}{dx}(1) = 0,$$

$$(67) \quad \Gamma = \begin{bmatrix} \gamma_1 \\ \gamma_2 \end{bmatrix} = G^{-1} \begin{bmatrix} -C_1 \tilde{z} + y_{r1} \\ -C_2 \tilde{z} + y_{r2} \end{bmatrix}.$$

Finally, we use the inputs  $\gamma_1$  and  $\gamma_2$  in (48)-(50) to obtain the controlled plant (43)-(50)

$$(68) \quad z_t = \nu z_{xx} - z z_x - \delta_{0.5} \gamma_1, \quad \text{for } 0 < x < 1 \text{ and } 0 < t \leq T$$

$$(69) \quad z(0, t) = d, \quad \nu z_x(1, t) = \gamma_2,$$

$$(70) \quad z(x, 0) = \varphi(x).$$

For this example we have chosen the parameters  $\nu = 0.2$ ,  $d = 0.75$ ,  $y_{r1} = 0.5$  and  $y_{r2} = 1$ .

After following step-by-step the procedure in Eqs. (57)-(67), and evaluating the inputs parameters,  $\gamma_1$  and  $\gamma_2$ , we solve the closed loop system (68)-(70) on the time interval  $0 < t \leq T$  with  $T = 10$  and initial data  $\varphi(x) = 0$ . The numerical solution of the weak formulation of the above three systems is obtained using the predefined PDE Coefficient tool of the COMSOL Multiphysics 3.5a package. The geometry is discretized with 128 quadratic Lagrange elements. No stabilization method is used for the advection term. In Figure 2, we display both the steady state solution  $\bar{z}(x)$  and the solution of the closed loop system  $z(x, t)$  at  $t = 10$ . As expected the two graphs nearly perfectly overlap, since  $\bar{z}(x)$  serves as a local attractor for  $z(x, t)$ . In Figure 3, the quantities  $C_1 z(t)$  and  $C_2 z(t)$  are given for all times. The asymptotic convergence of  $C_1 z(t)$  to  $y_{r1} = 0.5$  and  $C_2 z(t)$  to  $y_{r2} = 1$  is evident.

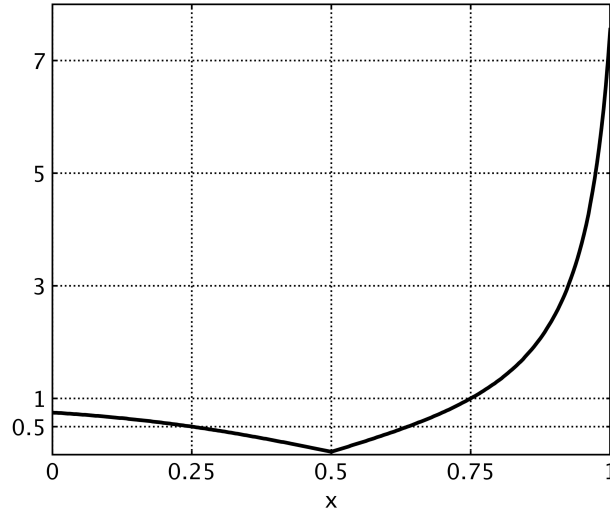


FIGURE 2. Steady state solution  $\bar{z}(x)$  and closed loop solution  $z(x,t)$  at  $t=10$ . As we anticipate, by time  $t = 10$  the two solutions cannot be distinguished and appear to be identical.

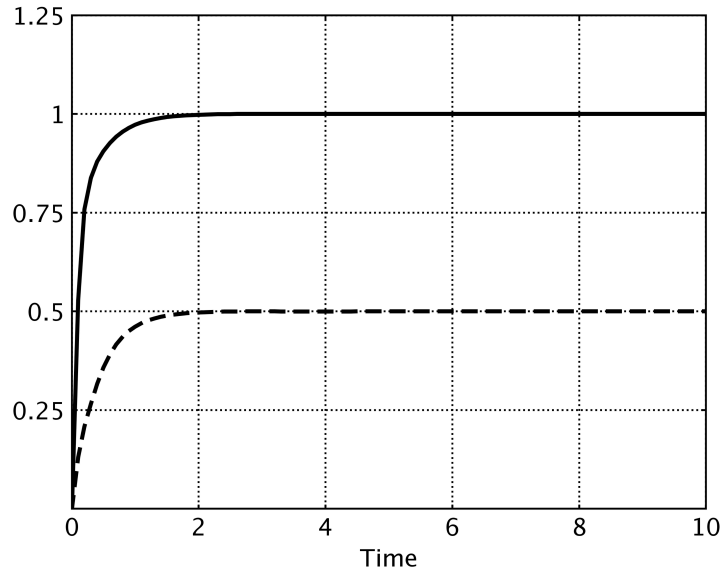


FIGURE 3.  $C_1z(t) = z(0.25,t)$  (dashed line) and  $C_2z(t) = z(0.75,t)$  (continuous line) for  $0 \leq t \leq 10$ .

In Figure 4 we display the solution profile  $z(x,t)$  both in space and time.

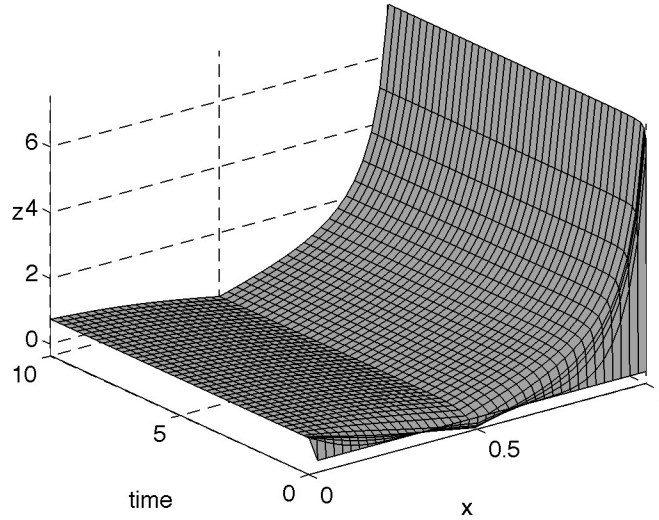


FIGURE 4. Solution  $z(x, t)$  for  $0 \leq x \leq 1$  and  $0 \leq t \leq 10$ .

In Figure 4 we note that at  $x = 0$  the numerical solution satisfies  $z(0, t) = 0.75$  and, as seen in Figure 3,  $z(0.25, t)$  and  $z(0.75, t)$  rapidly approach 0.5 and 1 as required.

**4.2. Navier-Stokes Flow in a Two Dimensional Forked Channel.** In this section, we consider the modeling and control of a two dimensional incompressible Navier-Stokes flow in a region  $\Omega$  described in Fig 5.

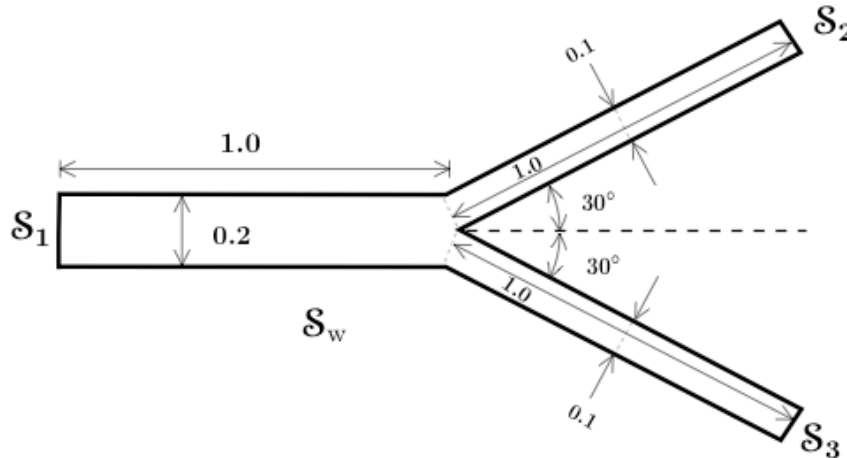


FIGURE 5. Forked Channel Domain.

The domain  $\Omega$  consists of a main channel of length 1 and altitude 0.2 which forks at the right extreme dividing into two equal branches of length 1 and altitude 0.1. The branches are inclined at  $30^\circ$  with respect to the main channel. The channel is

open on the left at  $\Gamma_1$  and on the right at  $\Gamma_2$  and  $\Gamma_3$ . Walls are considered on the remaining part of the boundary, denoted by  $\Gamma_w$ .

In the whole domain the incompressible Navier-Stokes system of equations is considered for some initial data  $\boldsymbol{\varphi}$ . There is a constant disturbance  $d$  entering through a parabolic inflow profile on the boundary  $\Gamma_1$  and a boundary control  $u$  entering through a normal stress on  $\Gamma_2$ . Zero stress and zero velocity boundary conditions are considered on  $\Gamma_3$  and  $\Gamma_w$ , respectively. We have a measured output on  $\Gamma_3$  given by the average velocity in the outward normal direction. Namely

$$(71) \quad \frac{\partial \mathbf{v}}{\partial t} + (\mathbf{v} \cdot \nabla) \mathbf{v} = \nabla \cdot (\nu [(\nabla \mathbf{v}) + (\nabla \mathbf{v})^\top]) - \nabla p,$$

$$(72) \quad \nabla \cdot \mathbf{v} = 0,$$

$$(73) \quad \mathbf{v}(x, 0) = \boldsymbol{\varphi}(x),$$

$$(74) \quad \mathbf{v}|_{\Gamma_1} = \begin{bmatrix} f(s)d \\ 0 \end{bmatrix},$$

$$(75) \quad \boldsymbol{\tau}(z)|_{\Gamma_2} = u \mathbf{n}_{\Gamma_2},$$

$$(76) \quad \boldsymbol{\tau}(z)|_{\Gamma_3} = \mathbf{0},$$

$$(77) \quad \mathbf{v}|_{\Gamma_w} = \mathbf{0},$$

$$(78) \quad y = C(z) = \frac{1}{|\Gamma_3|} \int_{\Gamma_3} \mathbf{v} \cdot \mathbf{n}_{\Gamma_3} ds.$$

Here  $z = (\mathbf{v}, p)$  is the state variable, where  $\mathbf{v} = [v_1, v_2]^\top$  denotes the velocity vector field and  $p$  the pressure. We also use the notations of  $\nu$  for the cinematic viscosity,

$$(79) \quad f(s) = 4s(1 - s)$$

for the parabolic inflow with maximum amplitude 1, where  $s$  is the arclength normalized between 0 and 1, and  $\boldsymbol{\tau}$  for the surface stress on  $\Gamma$  given by

$$(80) \quad \boldsymbol{\tau}(z) = (pI - \nu [(\nabla \mathbf{v}) + (\nabla \mathbf{v})^\top]) \cdot \mathbf{n}_\Gamma,$$

with  $\mathbf{n}_\Gamma = [n_x, n_y]^\top$  the outward normal on the boundary  $\Gamma$ .

Again, in this example, our objective is to find a control input  $u$  so that the measured output  $y(t)$  tracks a given reference signal  $y_r$  while rejecting the disturbance  $d$ .

The controller  $u$  is found by following the algorithm outlined in Section 3. First we solve the linear steady state Stokes problem for  $X = [\mathbf{V}, P]^\top$ , with homogeneous boundary condition everywhere except on  $\Gamma_2$ , where a unit normal stress is considered

$$(81) \quad \mathbf{0} = \nabla \cdot (\nu [(\nabla \mathbf{V}) + (\nabla \mathbf{V})^\top]) - \nabla P,$$

$$(82) \quad \nabla \cdot \mathbf{V} = 0,$$

$$(83) \quad \mathbf{V}|_{\Gamma_1} = \mathbf{0}, \quad \boldsymbol{\tau}(X)|_{\Gamma_3} = \mathbf{0}, \quad \mathbf{V}|_{\Gamma_w} = \mathbf{0},$$

$$(84) \quad \boldsymbol{\tau}(X)|_{\Gamma_2} = \mathbf{n}_{\Gamma_2}.$$

We note that  $X$  is the response of the homogeneous linear Stokes operator to the unit normal stress input on  $\Gamma_2$  and produces the entry of the  $1 \times 1$  matrix (i.e., a scalar in this case)

$$(85) \quad G = (C(X)).$$

With this we solve the coupled non-linear steady-state systems with unknowns  $\bar{z} = [\bar{v}, \bar{p}]$ ,  $\tilde{z} = [\tilde{v}, \tilde{p}]$  and  $\gamma$

$$(86) \quad \mathbf{0} = \nabla \cdot (\nu [(\nabla \bar{v}) + (\nabla \bar{v})^\top]) - (\bar{v} \cdot \nabla) \bar{v} - \nabla \bar{p},$$

$$(87) \quad \nabla \cdot \bar{v} = 0,$$

$$(88) \quad \bar{v}|_{\Gamma_1} = \begin{bmatrix} f(s)d \\ 0 \end{bmatrix}, \quad \bar{v}|_{\Gamma_w} = \mathbf{0},$$

$$(89) \quad \boldsymbol{\tau}(\bar{z})|_{\Gamma_2} = \gamma \mathbf{n}_{\Gamma_2}, \quad \boldsymbol{\tau}(\bar{z})|_{\Gamma_3} = \mathbf{0},$$

$$(90)$$

$$(91) \quad \mathbf{0} = \nabla \cdot (\nu [(\nabla \tilde{v}) + (\nabla \tilde{v})^\top]) - (\tilde{v} \cdot \nabla) \tilde{v} - \nabla \tilde{p},$$

$$(92) \quad \nabla \cdot \tilde{v} = 0,$$

$$(93) \quad \tilde{v}|_{\Gamma_1} = \begin{bmatrix} f(s)d \\ 0 \end{bmatrix}, \quad \tilde{v}|_{\Gamma_w} = \mathbf{0},$$

$$(94) \quad \boldsymbol{\tau}(\tilde{z})|_{\Gamma_2} = \mathbf{0}, \quad \boldsymbol{\tau}(\tilde{z})|_{\Gamma_3} = \mathbf{0},$$

$$(95) \quad \gamma = G^{-1}(y_r - C(\tilde{z})) = \frac{1}{C(X)}(y_r - C(\tilde{z})).$$

Finally we set  $u = \gamma$  and solve the IBVP (71)-(77) – the closed loop system. Under Assumptions 3.1 and 3.2 we expect  $z \rightarrow \bar{z}$ , for  $t \rightarrow \infty$ , in such a way that the desired tracking  $y(t) = C(z) \rightarrow C(\bar{z}) = y_r$  takes place.

For our specific numerical example we have chosen the following parameters:  $\nu = 0.002$ ,  $d = 1$  and  $y_r = 2$ . Accordingly, the maximum Reynolds number occurs in the lower branch and is

$$Re = \frac{y_r D}{\nu} = 100.$$

The initial data in our simulation is  $\boldsymbol{\varphi}(x) = \mathbf{0}$  and the transient solution  $z(x, t)$  is evaluated between  $t = 0$  and  $t = 5$ .

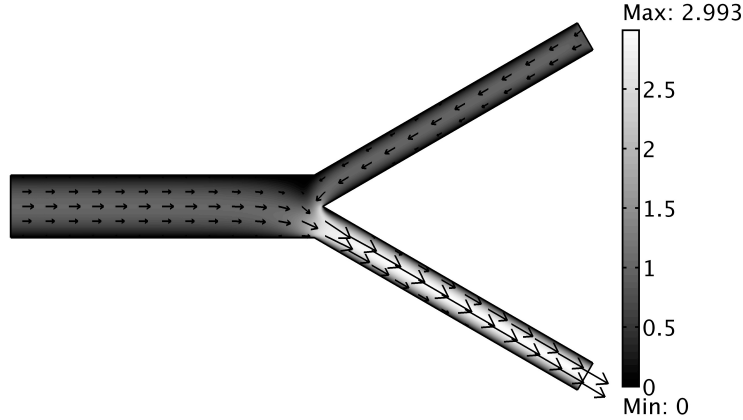


FIGURE 6. Vector field  $\mathbf{v}$  and its magnitude  $\|\mathbf{v}\|$  at  $T = 5$ .

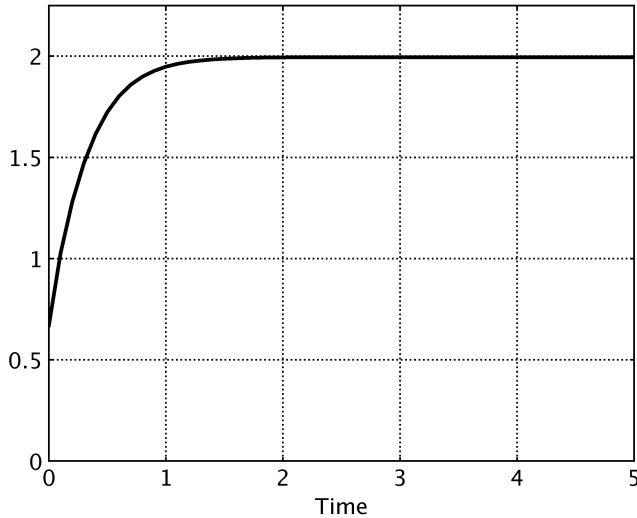


FIGURE 7.  $Cz(t)$  for  $0 \leq t \leq 5$ .

The numerical solution of the weak formulation of the above three systems is obtained using the predefined Navier-Stokes incompressible model of the COMSOL Multiphysics 3.5a package. Lagrange elements  $\mathbf{P2-P1}$  are used for velocity and pressure in order to satisfy the LBB condition. Stabilization of the advection term is obtained using streamline diffusion (GLS) and crosswind diffusion with coefficient  $C_k = 0.1$ . These are predefined parameters [7]. The geometry is discretized with a mesh of 17408 triangular elements. In Figure 6 a screen-shot of the vector field  $\mathbf{v}$  and its magnitude  $\|\mathbf{v}\|$  is given at time  $T = 5$ . The time evolution of  $Cz$  is given in Figure 7 for  $0 \leq t \leq 5$ . The asymptotic convergence of  $Cz(t)$  to  $y_r = 2$  is evident.

**Remark 4.2.** From a physical point of view the velocity vector field  $\mathbf{v}$  is generated by the difference between the normal stress components on  $\Gamma_2$  and  $\Gamma_3$ . Any combination of two control inputs  $u_1$  and  $u_2$  such that

$$(96) \quad \boldsymbol{\tau}(z)|_{\Gamma_2} = u_1 \mathbf{n}_{\Gamma_2},$$

$$(97) \quad \boldsymbol{\tau}(z)|_{\Gamma_3} = u_2 \mathbf{n}_{\Gamma_3},$$

$$(98) \quad u_1 - u_2 = \gamma,$$

would give exactly the same velocity vector field  $\mathbf{v}$ , while a shift of  $u_2$  in the pressure profile would occur. Consequently  $Cz(t)$  would not change. Among all the possible combinations of  $u_1$  and  $u_2$  satisfying constraint (98), the one having the least Euclidean norm is, clearly,

$$(99) \quad u_1 = -u_2 = \frac{\gamma}{2}.$$

Let us reconsider the same control problem described in Eqs. (71) – (78), where the boundary conditions (75) and (76) on  $\Gamma_2$  and  $\Gamma_3$  are replaced with Eqs. (96) and (97), respectively. The resulting system has now two control inputs and one measured output.

The controls  $u_1$  and  $u_2$  are found by following again the procedure described in Section 3. We want to show that in case of multiple solutions this procedure will return the solution having the least Euclidean norm, namely Eq. (99).

First we determine  $X_1$  and  $X_2$  as the responses of the homogeneous linear Stokes operator to unit normal stresses on  $\Gamma_2$  and  $\Gamma_3$ . Note that  $X_1$  is exactly the solution  $X = [\mathbf{V}, P]^\top$  previously evaluated by solving system (81) – (84), while  $X_2 = [\mathbf{V}_2, P_2]^\top$  solves

$$(100) \quad \mathbf{0} = \nabla \cdot (\nu [(\nabla \mathbf{V}_2) + (\nabla \mathbf{V}_2)^\top]) - \nabla P_2,$$

$$(101) \quad \nabla \cdot \mathbf{V}_2 = 0,$$

$$(102) \quad \mathbf{V}_2|_{\Gamma_1} = \mathbf{0}, \quad \boldsymbol{\tau}(X_2)|_{\Gamma_2} = \mathbf{0}, \quad \mathbf{V}_2|_{\Gamma_w} = \mathbf{0},$$

$$(103) \quad \boldsymbol{\tau}(X_2)|_{\Gamma_3} = \mathbf{n}_{\Gamma_3}.$$

According to Remark 4.2 and the linearity of the problem, we must have  $X_2 = -[\mathbf{V}, P - 1]^\top$ . In this case the new  $1 \times 2$  matrix  $G$  is given by

$$(104) \quad G = (CX_1, CX_2) = CX(1, -1).$$

We now obtain  $\bar{z}$  and  $\tilde{z}$  by solving the system (86)-(95), where Eqs. (89) and (95) are replaced by

$$(105) \quad \boldsymbol{\tau}(\bar{z})|_{\Gamma_2} = \gamma_1 \mathbf{n}_{\Gamma_2}, \quad \boldsymbol{\tau}(\bar{z})|_{\Gamma_3} = \gamma_2 \mathbf{n}_{\Gamma_2},$$

$$(106) \quad \Gamma = \begin{bmatrix} \gamma_1 \\ \gamma_2 \end{bmatrix} = G^+(y_r - C\tilde{z}) = \frac{1}{CX} \begin{bmatrix} 0.5 \\ -0.5 \end{bmatrix} (y_r - C\tilde{z}),$$

respectively. Here  $G^+$  is the pseudoinverse of  $G$ . It is not difficult to see that the solution of this new system is given by  $\bar{z} = [\bar{\mathbf{v}}, \bar{p} - \gamma_2]^\top$ ,  $\tilde{z} = [\tilde{\mathbf{v}}, \tilde{p}]^\top$  and  $\gamma_1 = -\gamma_2 = \gamma/2$ , where the quantities  $\bar{\mathbf{v}}$ ,  $\bar{p}$ ,  $\tilde{\mathbf{v}}$ ,  $\tilde{p}$  and  $\gamma$  were previously evaluated solving the original system (86)-(95). Finally we choose  $u_1 = \gamma_1$  and  $u_2 = \gamma_2$  for the closed loop system. This is exactly Eq. (99). According to Remark 4.2 the time dependent solution  $z$  is given by  $z = [\mathbf{v}, P - \gamma/2]^\top$ , thus  $Cz$  remains the same. With this simple example, we have shown that the use of the pseudoinverse in Eq. (106) returns, as expected, the solution having the least Euclidean norm. The numerical solution of the modified system is identical to the original one, with the only exception that, as expected, the original pressure has been shifted of  $-\gamma/2$ .

**4.3. Non-Isothermal Navier-Stokes Flow in a Two Dimensional Box Domain.** In this section, we consider the modeling and control of a two dimensional non-isothermal Navier-Stokes flow in the region  $\Omega$  described in Fig 8. The motivation for considering this example comes from discussions with researchers at Virginia Tech University actively engaged in research directed in part at control problems in the design of energy efficient buildings.

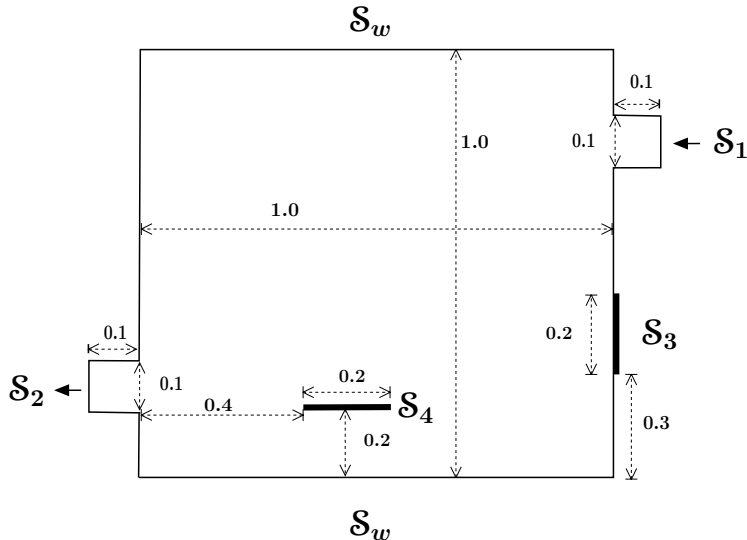


FIGURE 8. Two Dimensional Box Domain.

The domain  $\Omega$  consists of a main square box with side length 1. Inlet and outlet square regions, of side length 0.1, are located on the upper-right and lower-left sides of the main box, respectively. The boundary of the region  $\Omega$  consists of an inflow boundary  $\Gamma_1$ , an outflow boundary  $\Gamma_2$  and a hot wall  $\Gamma_3$ . Insulated walls are considered on the rest of the boundary  $\Gamma_w$ . A solid interior wall boundary is also considered at  $\Gamma_4$ .

The physical model governing this problem consists of the non-isothermal incompressible Navier-Stokes equations in the entire domain. In the momentum equation we use the Boussinesq approximation to describe the buoyancy force. There is a boundary control  $u$  entering through a distributed heat flux on  $\Gamma_1$ , and a disturbance  $d$  entering on the wall  $\Gamma_3$  through a constant given temperature. A parabolic inflow profile is considered for the fluid velocity on  $\Gamma_1$ . Zero stress and zero flux boundary conditions are considered on  $\Gamma_2$ , while zero velocity and zero flux are considered on  $\Gamma_w$ . The wall  $\Gamma_4$  is an interior boundary only in the momentum equation; it is part of the domain in the temperature equation. In other words, since the thickness of  $\Gamma_4$  is considered to be zero, the wall effects on  $\Gamma_4$  enter in the temperature equation through the advection term only, rather than as boundary conditions or sink/source terms. We have a measured output on  $\Gamma_4$  given by the average temperature.

Formulating the above within a mathematical framework we have,

$$(107) \quad \frac{\partial \mathbf{v}}{\partial t} + (\mathbf{v} \cdot \nabla) \mathbf{v} = \nabla \cdot (\nu [(\nabla \mathbf{v}) + (\nabla \mathbf{v})^\top]) - \nabla p + \beta T,$$

$$(108) \quad \nabla \cdot \mathbf{v} = 0,$$

$$(109) \quad \frac{\partial T}{\partial t} + (\mathbf{v} \cdot \nabla) T = \alpha \Delta T,$$

with initial data

$$(110) \quad \mathbf{v}(x, 0) = \boldsymbol{\varphi}(x), \quad T(x, 0) = \phi(x),$$

boundary conditions

$$(111) \quad \mathbf{v} = \begin{bmatrix} f(s) \\ 0 \end{bmatrix} \quad \text{and} \quad \mathbf{q} = u \mathbf{n}_{\Gamma_1} \quad \text{on} \quad \Gamma_1,$$

$$(112) \quad \boldsymbol{\tau} = \mathbf{0} \quad \text{and} \quad \mathbf{q} = \mathbf{0} \quad \text{on} \quad \Gamma_2,$$

$$(113) \quad \mathbf{v} = \mathbf{0} \quad \text{and} \quad T = d \quad \text{on} \quad \Gamma_3,$$

$$(114) \quad \mathbf{v} = \mathbf{0} \quad \text{and} \quad \mathbf{q} = \mathbf{0} \quad \text{on} \quad \Gamma_w,$$

$$(115) \quad \mathbf{v} = \mathbf{0} \quad \text{on} \quad \Gamma_4,$$

and measured output

$$(116) \quad y = C(z) = \frac{1}{|\Gamma_4|} \int_{\Gamma_4} T ds.$$

Here  $z = (\mathbf{v}, p, T)$  is the state variable, where  $\mathbf{v} = [v_1, v_2]^\top$  denotes the velocity vector field,  $p$  the pressure and  $T$  the temperature. We also use the notations of  $\nu$  for the cinematic viscosity,  $\alpha$  for the thermal diffusivity,  $\beta$  for the buoyancy coefficient, and

$$(117) \quad f(s) = 4s(1 - s)$$

for the parabolic inflow with maximum amplitude 1, where  $s$  is the arclength normalized between 0 and 1. The surface stress  $\boldsymbol{\tau}$  and the heat flux  $\mathbf{q}$  on  $\Gamma$  are given, respectively, by

$$(118) \quad \boldsymbol{\tau}(\mathbf{v}, p) = (pI - \nu [(\nabla \mathbf{v}) + (\nabla \mathbf{v})^\top]) \cdot \mathbf{n}_\Gamma,$$

$$(119) \quad \mathbf{q}(T) = -\alpha \nabla T \cdot \mathbf{n}_\Gamma,$$

with  $\mathbf{n}_\Gamma = [n_x, n_y]^\top$  the outward normal on the boundary  $\Gamma$ .

Again, in this example, our objective is to find a control input  $u$  so that the measured output  $y(t)$  tracks a given (constant) reference signal  $y_r$  while rejecting the disturbance  $d$ . The controller  $u$  is found by proceeding as described in the Section 3. We notice that the momentum equation is coupled to the temperature only through the buoyancy term. We first determine the steady state velocity in absence of buoyancy force by solving the isothermal Navier-Stokes equation

$$(120) \quad (\mathbf{V} \cdot \nabla) \mathbf{V} = \nabla \cdot (\nu [(\nabla \mathbf{V}) + (\nabla \mathbf{V})^\top]) - \nabla P,$$

$$(121) \quad \nabla \cdot \mathbf{V} = 0,$$

$$(122) \quad \mathbf{V} = \begin{bmatrix} f(s) \\ 0 \end{bmatrix} \quad \text{on} \quad \Gamma_1,$$

$$(123) \quad \boldsymbol{\tau} = \mathbf{0} \quad \text{on} \quad \Gamma_2,$$

$$(124) \quad \mathbf{V} = \mathbf{0} \quad \text{on} \quad \Gamma_3 \cup \Gamma_w \cup \Gamma_4.$$

for the variable  $\mathbf{V}$  and  $P$ . Then we solve the linear energy equation for  $X$ , with homogeneous boundary condition everywhere except on  $\Gamma_1$ , where a unit heat flux is considered

$$(125) \quad 0 = \alpha \Delta X - (\mathbf{V} \cdot \nabla) X,$$

$$(126) \quad \mathbf{q} = 1 \mathbf{n}_{\Gamma_1} \quad \text{on} \quad \Gamma_1,$$

$$(127) \quad \mathbf{q} = \mathbf{0} \quad \text{on} \quad \Gamma_2 \cup \Gamma_w,$$

$$(128) \quad X = 0 \quad \text{on} \quad \Gamma_3.$$

Here  $X$  is the response of the homogeneous energy equation to the unit input on  $\Gamma_1$ , and produces the entry of the  $1 \times 1$  matrix (i.e., a scalar in this case)

$$(129) \quad G = (C(X)).$$

**Remark 4.3.** In the previous system Eq. (125) is linear, since the advection velocity  $\mathbf{V}$  is given. In the energy equation we then consider the linear homogeneous operator  $A$  applied to the state variable  $X$  to be given by  $\alpha\Delta X - (\mathbf{V} \cdot \nabla)X$  rather than  $\alpha\Delta X$ , only. Again we assume  $\mathbf{V}$  to be so that  $A$  is always invertible. Here, of course, the definition of the linear operator  $A$  is also supplemented by the homogeneous boundary conditions on the boundary of the domain  $\Omega$ . The above choice of  $A$  is motivated by the fact that in the current example we expect the flow to be mostly driven by the inflow boundary condition rather than the buoyancy force. Under this assumption we included in  $A$  what we expect to be a good approximation of the advection term. Thus, considering both diffusion and convection in the linear operator gives a more realistic response than considering diffusion only.

With this we solve now the fully coupled non-linear steady-state system

$$(130) \quad (\bar{\mathbf{v}} \cdot \nabla)\bar{\mathbf{v}} = \nabla \cdot (\nu[(\nabla\bar{\mathbf{v}}) + (\nabla\bar{\mathbf{v}})^\top]) - \nabla\bar{p} + \beta\bar{T},$$

$$(131) \quad \nabla \cdot \bar{\mathbf{v}} = 0,$$

$$(132) \quad (\bar{\mathbf{v}} \cdot \nabla)\bar{T} = \alpha\Delta\bar{T},$$

$$(133) \quad ((\bar{\mathbf{v}} - \mathbf{V}) \cdot \nabla)\bar{T} = \alpha\Delta\tilde{T} - (\mathbf{V} \cdot \nabla)\tilde{T},$$

with boundary conditions

$$(134) \quad \bar{\mathbf{v}} = \begin{bmatrix} f(s) \\ 0 \end{bmatrix}, \quad \mathbf{q}(\bar{T}) = \gamma \mathbf{n}_{\Gamma_1} \text{ and } \mathbf{q}(\tilde{T}) = \mathbf{0} \text{ on } \Gamma_1,$$

$$(135) \quad \boldsymbol{\tau}(\bar{\mathbf{v}}, \bar{p}) = \mathbf{0}, \quad \mathbf{q}(\bar{T}) = \mathbf{0} \text{ and } \mathbf{q}(\tilde{T}) = \mathbf{0} \text{ on } \Gamma_2,$$

$$(136) \quad \bar{\mathbf{v}} = \mathbf{0}, \quad \bar{T} = d \text{ and } \tilde{T} = d \text{ on } \Gamma_3,$$

$$(137) \quad \bar{\mathbf{v}} = \mathbf{0}, \quad \mathbf{q}(\bar{T}) = \mathbf{0} \text{ and } \mathbf{q}(\tilde{T}) = \mathbf{0} \text{ on } \Gamma_w,$$

$$(138) \quad \bar{\mathbf{v}} = \mathbf{0} \text{ on } \Gamma_4,$$

and control

$$(139) \quad \gamma = G^{-1}(y_r - C(\tilde{T})) = \frac{1}{C(X)}(y_r - C(\tilde{T})).$$

Finally we set  $u = \gamma$  and solve the IBVP (107)-(115). Under Assumptions 3.1 and 3.2 we expect  $T \rightarrow \bar{T}$ , for  $t \rightarrow \infty$ , so that, in addition, the desired tracking  $y(t) = C(T) \rightarrow C(\bar{T}) = y_r$  takes place.

For our specific numerical example we have chosen the following parameters:  $\nu = 0.002$ ,  $\alpha = 0.01$ ,  $\beta = 1.$ ,  $d = 1.$  and  $y_r = 0.5$ . Accordingly, the maximum Reynolds number occurs in the inlet region and is approximately  $Re \simeq 250$ . The Prandtl and Grashof numbers are

$$(140) \quad Pr = \frac{\nu}{\alpha} = 0.2, \quad Gr = \frac{\beta y_r D^3}{\nu^2} = 1.25 \times 10^5,$$

respectively. The initial data in our simulation are  $\boldsymbol{\varphi}(x) = \mathbf{0}$  and  $\phi(x) = 0$ . The transient solution  $z(x, t)$  is evaluated between  $t = 0$  and  $t = 2000$ . The numerical solution of the weak formulation of the above systems is obtained with the COMSOL Multiphysics 3.5a package. The momentum and continuity equations are solved using the predefined Navier-Stokes incompressible model. The energy equation is solved by using the PDE coefficient model. In the Navier-Stokes model Lagrange

elements  $P2-P1$  are used for velocity and pressure in order to satisfy the LBB condition. Stabilization of the advection term is obtained using streamline diffusion (GLS) and crosswind diffusion with coefficient  $C_k = 0.1$ . These are predefined parameters [7]. In the PDE coefficient model Lagrange elements  $P2$  are used for the Temperature. No stabilization is used for the advection term. The geometry is discretized with a mesh of 8976 triangular elements. In Figure 9 a screen-shot of the velocity vector field  $\mathbf{v}$  and the temperature profile  $T$  is given. In Figure 10 we show the velocity magnitude  $\|\mathbf{v}\|$  and streamlines at the final time  $t = 2000$ . The time evolution of  $CT$  is given in Figure 11 for all time (solid line). The asymptotic convergence of  $CT(t)$  to  $y_r = 0.5$  is again evident.

**Remark 4.4.** In this example we have used a flux boundary control on  $\Gamma_1$ . A Dirichlet boundary control can also be found to reach the desired output  $y_r$ . For example, a constant temperature value  $u$  on the inlet boundary

$$(141) \quad T = u \text{ on } \Gamma_1,$$

can be obtained by proceeding as described in the Section 3.

Alternatively, a Dirichlet boundary control can be easily found by using the information already gained solving the flux boundary control problem. In particular the trace of  $\bar{T}$  on the boundary  $\Gamma_1$  can be used in the closed loop system as a Dirichlet controller

$$(142) \quad T = \bar{T} \text{ on } \Gamma_1.$$

The time evolution of  $CT(t)$  in this case is given by the dashed line in Figure 11. The two transients are different, but the asymptotic values are clearly the same.

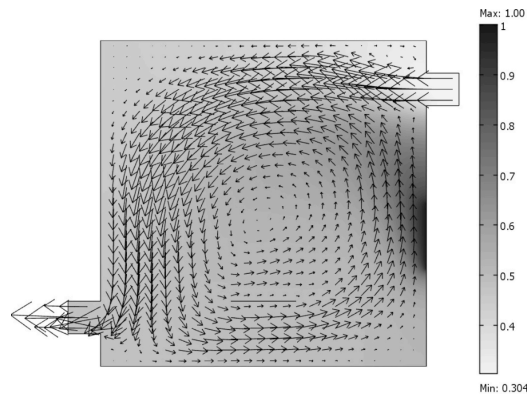


FIGURE 9. Velocity vector field  $\mathbf{v}$  and temperature profile  $T$

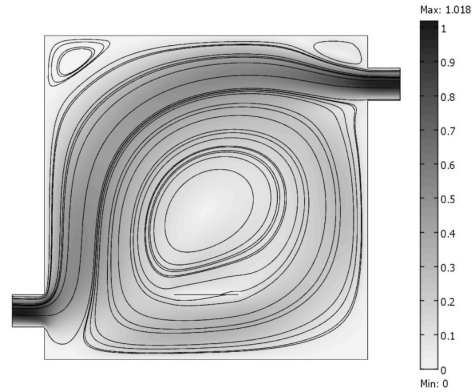


FIGURE 10. Velocity magnitude profile  $\|\mathbf{v}\|$  and velocity streamlines at  $t = 2000$ .

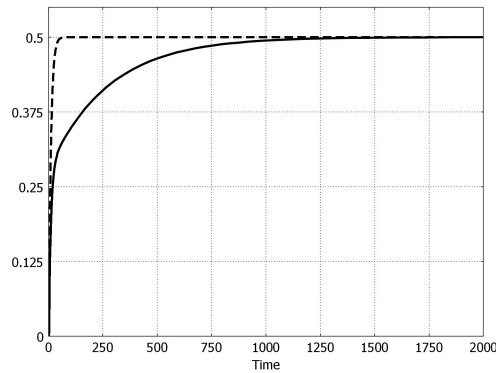


FIGURE 11. Time evolution of  $CT$  for the flux control case (solid line) and the Dirichlet control case (dashed line) for all time.

## 5. The time dependent case

In this last section we briefly discuss a general strategy to track and reject piecewise constant time dependent signals, when the inertial terms are not negligible. We will see that a slightly modification of the procedure described in Section 3 can be adopted to achieve the desired goals, however some numerical instabilities occur and a certain approximation in the algorithm is required. A more general and detailed description for the time dependent case, with no approximation, is the focus of a forthcoming paper [1].

In this section, rather than treating constant reference signals and disturbances, let us consider the more general problem

$$(143) \quad z_t(x, t) = Az(x, t) + F(z(x, t)) + \sum_{j=0}^{n_d} \Theta_j(x) d_j(t) + \sum_{j=0}^{n_{in}} \Phi_j(x) u_j(t),$$

$$(144) \quad z(x, 0) = z_0(x), \quad z_0 \in \mathcal{Z} = L^2(\Omega),$$

$$(145) \quad y_i(t) = (C_i z)(t), \quad i = 1, \dots, n_c.$$

Our goal is to find time dependent controllers  $u_j(t) = \gamma_j(t)$ , in order to track and reject piecewise constant time dependent signals  $y_{r_i}(t)$  and  $d_j(t)$ . As a first approximation since  $y_{r_i}(t)$  and  $d_j(t)$  are piecewise constant in time, we could split the time interval into sub-intervals  $0 = t_0, t_1, \dots, t_N$ , such that both  $y_{r_i}(t)$  and  $d_j(t)$  are constant on each sub-interval, i.e.,

$$(146) \quad y_{r_i}(t) = y_{r_{i,k}} \quad \text{and} \quad d_j(t) = d_{j,k}, \quad \text{for } t \in [t_k, t_{k+1}).$$

Then, according to Section 3, for the  $k$ th sub-interval, we can find a set of controllers  $\gamma_{j,k}$ , and build piecewise time dependent controllers

$$(147) \quad u_j(t) = \gamma_{j,k}, \quad \text{for } t \in [t_k, t_{k+1}).$$

Using this procedure, we find that any time  $y_{r_i}(t)$  or  $d_j(t)$  changes a transient with

$$y_{r_i}(t) \neq y_i(t) = (C_i z)(x)$$

occurs. As long as the inertial terms remain small, the error is quickly reabsorbed. However, if the inertial terms are not negligible then we need to take into account their effect in the controller evaluation strategy.

In the latter case, in order to determine the controllers  $\gamma_j(t)$  we proceed by following a procedure similar to the one described in Section 3 with the exception that we consider the auxiliary state variables  $\bar{z}$  are  $\tilde{z}$  to be now time dependent.

We use as initial data for  $\bar{z}(x, 0)$  the steady state solutions  $\bar{Z}(x)$  needed to solve the set point control problem

$$(148) \quad Z(x, t) = AZ(x, t) + F(Z(x, t)) + \sum_{j=0}^{n_d} \Theta_j(x) d_{j,0} + \sum_{j=0}^{n_{in}} \Phi_j(x) \gamma_{j,0},$$

$$(149) \quad Z(x, 0) = z_0(x),$$

$$(150) \quad y_i(t) = (C_i Z)(t), \quad i = 1, \dots, n_c,$$

where the disturbances and the signals to be tracked are

$$(151) \quad d_{j,0} = d_j(0), \quad y_{r_{i,0}} = y_{r_i}(0),$$

respectively. Thus, they are time *independent*. Notice that to find  $Z(x)$ , we follow the strategy described in Section 3, and determine the solutions  $X_j$ , the matrix  $G$  and the controllers  $u_{j,0} = \gamma_{j,0}$ , however there is no need to solve for the close loop system (148)-(150).

Next we seek controllers  $u_j(t) = \gamma_j(t)$  such that  $\bar{z}(x, t)$  satisfy

$$(152) \quad \bar{z}_t(x, t) = A\bar{z}(x, t) + F(\bar{z}(x, t)) + \sum_{j=0}^{n_d} \Theta_j(x) d_j(t) + \sum_{j=0}^{n_{in}} \Phi_j(x) \gamma_j(t),$$

$$(153) \quad \bar{z}(x, 0) = \bar{Z}(x),$$

$$(154) \quad y_{r_i}(t) = (C_i \bar{z})(t), \quad i = 1, \dots, n_c,$$

for all time. Notice that, because of the initial condition (153), Eq. (154) is automatically satisfied for  $t = 0$ .

We rewrite Eq. (152) as

$$(155) \quad \bar{z}(x, t) = -A^{-1} \left( -\bar{z}_t(x, t) + F(\bar{z}(x, t)) + \sum_{j=0}^{n_d} \Theta_j(x) d_j(t) \right) + \sum_{j=0}^{n_{in}} (-A^{-1} \Phi_j(x) \gamma_j(t)).$$

Let  $\tilde{z}(x, t)$  be the solution of

$$(156) \quad \bar{z}_t(x, t) = A\tilde{z}(x, t) + F(\bar{z}(x, t)) + \sum_{j=0}^{n_d} \Theta_j(x) d_j(t).$$

Here,  $\tilde{z}$  is the response of the linear operator  $A$  to the sum of the nonlinear term  $F(\bar{z}(x))$ , the inertial term  $-\bar{z}_t(x, t)$  and all the disturbances  $\Theta_j d_j$ , namely

$$(157) \quad \tilde{z}(x, t) = -A^{-1} \left( F(\bar{z}(x, t)) - \bar{z}_t(x, t) + \sum_{j=0}^{n_d} \Theta_j(x) d_j(t) \right).$$

Substituting Eqs. (36) and (156) in Eq. (155) yields

$$(158) \quad \bar{z}(x, t) = \tilde{z}(x, t) + \sum_{j=0}^{n_{in}} X_j \gamma_j(t).$$

Applying the operator  $C_i$  to each side of the above equation, and substituting Eqs. (154) and (35) it follows that

$$(159) \quad (C_i \bar{z})(t) = (C_i \tilde{z})(t) + \sum_{j=0}^{n_{in}} g_{ij} \gamma_j(t) = y_{r_i}(t), \quad i = 1, \dots, n_c.$$

The above equation in matrix form is equivalent to

$$(160) \quad G\Gamma(t) = Y_r(t) - \tilde{Y}(t),$$

where  $\Gamma(t) = [\gamma_1(t), \gamma_2(t), \dots, \gamma_{n_{in}}(t)]^\top$ ,  $Y_r(t) = [y_{r_1}(t), y_{r_2}(t), \dots, y_{r_{n_c}}(t)]^\top$ , and  $\tilde{Y}(t) = [(C_1 \tilde{z})(t), (C_2 \tilde{z})(t), \dots, (C_{n_c} \tilde{z})(t)]^\top$ .

The initial boundary value problem (152)-(154), Eq. (156), and the coupling condition (160) should be solved together for all time. Once the controllers  $u_j(t) = \gamma_j(t)$  are known, they can be used in the closed loop system (143)-(145).

**Remark 5.1.** The system of equations (152)-(154), (156) represents a singular DAE and we have observed that introducing the inertial term in Eqs. (152) and (156) leads to numerical instabilities. Further, since there is no inertial term involving  $\tilde{z}_t(x, t)$  we see that although  $\tilde{z}$  is time dependent the solution of (156) does not require any initial data for  $\tilde{z}$ . In order to deal with the numerical instability we have found that slightly reducing the inertial effects of  $\bar{z}_t(x, t)$  in (156) produces a stable numerical system. Although this leads to an approximate solution for  $\bar{z}(x, t)$ , and therefore to

$$(161) \quad y_{r_i}(t) \simeq (C_i \bar{z})(t), \quad i = 1, \dots, n_c,$$

in most of the cases this error is very small, and is immediately reabsorbed.

Replacing the coefficient of  $\bar{z}_t(x, t)$  by  $(1 - \beta)$ , for small  $\beta > 0$ , the system (152)-(154), (156) becomes

$$(162) \quad \bar{z}_t(x, t) = A\bar{z}(x, t) + F(\bar{z}(x, t)) + \sum_{j=0}^{n_d} \Theta_j(x) d_j(t) + \sum_{j=0}^{n_{in}} \Phi_j(x) \gamma_j(t),$$

$$(163) \quad (1 - \beta)\bar{z}_t(x, t) = A\bar{z}(x, t) + F(\bar{z}(x, t)) + \sum_{j=0}^{n_d} \Theta_j(x) d_j(t),$$

$$(164) \quad \bar{z}(x, 0) = \bar{Z}(x),$$

$$(165) \quad y_{r_i}(t) = (C_i \bar{z})(t), \quad i = 1, \dots, n_c.$$

In our numerical simulation in the next section we have set  $\beta = .05$  which seems to work quite well. A detailed derivation of the errors for time dependent signals will be discussed in a forthcoming paper [1].

**5.1. A Numerical Example: Burgers' Equation.** In this section, we present an example of tracking piecewise constant references for a one dimensional Burgers' equation. This example is very similar to the Burgers' example presented in Section 4.1.

Consider the following control problem

$$(166) \quad z_t(x, t) = \nu z_{xx}(x, t) - z(x, t)z_x(x, t) + \delta_{0.5}u_1(t), \quad 0 \leq x \leq 1,$$

with initial data

$$(167) \quad z(x, 0) = \varphi(x),$$

boundary conditions

$$(168) \quad z(0, t) = d(t),$$

$$(169) \quad \nu z_x(1, t) + \alpha z(1, t) = u_2(t),$$

and measured outputs given by

$$(170) \quad y_1(t) = C_1(z) = z(0.25, t),$$

$$(171) \quad y_2(t) = C_2(z) = z(0.75, t).$$

With respect to the example discussed in Section 4.1, the disturbance  $d(t)$  is now a piecewise constant time dependent function, and the flux boundary condition on the right of the domain has been replaced by a (more stable) mixed boundary condition. Also the reference signals to track,  $y_{r_1}(t)$  and  $y_{r_2}(t)$ , are now piecewise constant time dependent functions.

Our objective is to find two control inputs  $u_j(t)$  with  $j = 1, 2$  so that the measured outputs  $y_j(t)$  track the reference signals  $y_{r_j}(t)$  while rejecting the disturbance  $d(t)$ .

The above description of the problem is illustrated in the Figure 12.

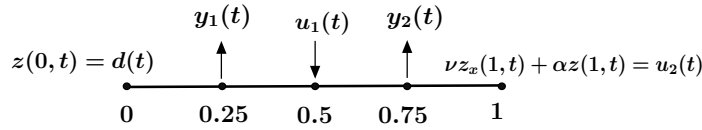


FIGURE 12. Burgers' example domain.

From here the problem is solved numerically by proceeding exactly as described in the first part of Section 5. First we must solve for  $X_j$  ( $j = 1, 2$ ), in steady-state problems

$$(172) \quad \nu \frac{d^2 X_1}{dx^2} = \delta_{0.5}, \quad \text{for } 0 < x < 1$$

$$(173) \quad X_1(0) = 0, \quad \nu \frac{dX_1}{dx}(1) + \alpha X_1(1) = 0,$$

for  $X_1$ , and

$$(174) \quad \nu \frac{d^2 X_2}{dx^2} = 0, \quad \text{for } 0 < x < 1,$$

$$(175) \quad X_2(0) = 0, \quad \nu \frac{dX_1}{dx}(1) + \alpha X_1(1) = 1,$$

for  $X_2$ . These produce the entries of the  $2 \times 2$  matrix

$$(176) \quad G = \begin{pmatrix} C_1 X_1 & C_1 X_2 \\ C_2 X_1 & C_2 X_2 \end{pmatrix}.$$

Then, we solve the steady state coupled system

$$(177) \quad 0 = \nu \frac{d^2 \bar{Z}}{dx^2} - \bar{Z} \frac{d\bar{Z}}{dx} - \delta_{0.5} \gamma_{1,0},$$

$$(178) \quad \bar{Z}(0) = d_0, \quad \nu \frac{d\bar{Z}}{dx}(1) + \alpha \bar{Z}(1) = \gamma_{2,0},$$

$$(179) \quad 0 = \nu \frac{d^2 \tilde{Z}}{dx^2} - \tilde{Z} \frac{d\tilde{Z}}{dx},$$

$$(180) \quad \tilde{Z}(0) = d_0, \quad \nu \frac{d\tilde{Z}}{dx}(1) + \alpha \tilde{Z}(1) = 0,$$

$$(181) \quad \Gamma = \begin{bmatrix} \gamma_{1,0} \\ \gamma_{2,0} \end{bmatrix} = G^{-1} \begin{bmatrix} -C_1 \tilde{Z} + y_{r_{1,0}} \\ -C_2 \tilde{Z} + y_{r_{2,0}} \end{bmatrix},$$

where  $d_0 = d(0)$ ,  $y_{r_{1,0}} = y_{r_1}(t)$  and  $y_{r_{2,0}} = y_{r_2}(t)$ . With this, we now solve the initial boundary value problem

$$(182) \quad \bar{z}_t = \nu \frac{d^2 \bar{z}}{dx^2} - \bar{z} \frac{d\bar{z}}{dx} - \delta_{0.5} \gamma_1(t),$$

$$(183) \quad \bar{z}(x, 0) = Z(x),$$

$$(184) \quad \bar{z}(0, t) = d(t), \quad \nu \frac{d\bar{z}}{dx}(1, t) + \alpha \bar{z}(1, t) = \gamma_2(t),$$

$$(185) \quad 0.95 \bar{z}_t = \nu \frac{d^2 \tilde{z}}{dx^2} - \tilde{z} \frac{d\tilde{z}}{dx},$$

$$(186) \quad \tilde{z}(0, t) = d(t), \quad \nu \frac{d\tilde{z}}{dx}(1, t) + \alpha \tilde{z}(1, t) = 0,$$

$$(187) \quad \Gamma = \begin{bmatrix} \gamma_1(t) \\ \gamma_2(t) \end{bmatrix} = G^{-1} \begin{bmatrix} -(C_1 \tilde{z})(t) + y_{r_1}(t) \\ -(C_2 \tilde{z})(t) + y_{r_2}(t) \end{bmatrix},$$

Finally, we set  $u_1(t) = \gamma_1(t)$  and  $u_2(t) = \gamma_2(t)$  and solve the close loop system (166)-(171).

For this example we choose the parameters  $\nu = 0.2$  and  $\alpha = 1000$ . Moreover, we set

$$(188) \quad d(t) = 0.75 + 0.25 U(t - 50) - 0.25 U(t - 100),$$

$$(189) \quad y_{r_1}(t) = 1 - 0.25 U(t - 25) + 0.5 U(t - 75) - 0.25 U(t - 125),$$

$$(190) \quad y_{r_2}(t) = 0.5 - 0.25 U(t - 40) + 0.5 U(t - 90) - 0.25 U(t - 140),$$

with  $U$  the Heaviside function defined by

$$(191) \quad U(x - x_0) = \begin{cases} 0 & \text{for } x < x_0, \\ 1 & \text{for } x \geq x_0. \end{cases}$$

For our numerical simulation we solve on the time interval  $0 < t \leq T$  with  $T = 150$  and initial data  $\varphi(x) = 0$ . The numerical solution of the weak formulation of the above systems is obtained using the predefined PDE Coefficient tool of the COMSOL Multiphysics 3.5a package. The geometry is discretized with 128 quadratic Lagrange elements. No stabilization method is used for the advection term.

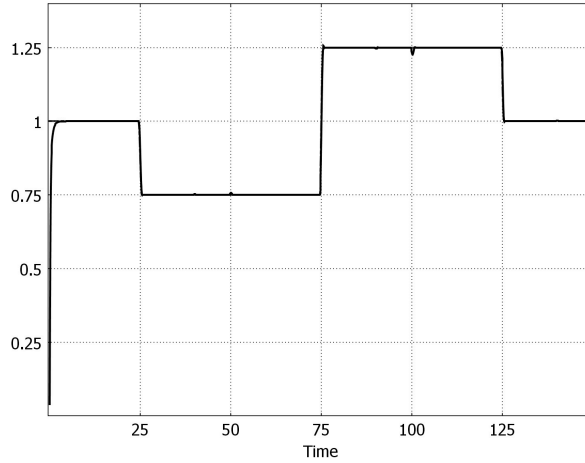


FIGURE 13.  $y_{r_1}(t)$  and  $(C_1 z)(t)$  for  $0 \leq t \leq 150$ .

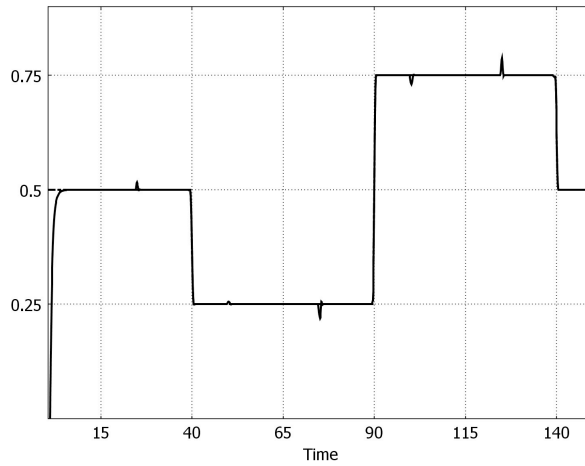


FIGURE 14.  $y_{r_2}(t)$  and  $(C_2 z)(t)$  for  $0 \leq t \leq 150$ .

In Figures 13, we display the reference signals  $y_{r_1}(t)$  and  $y_{r_2}(t)$  and the quantities  $(C_1 z)(t)$  and  $(C_2 z)(t)$  for all the time  $T$ . After a short transient  $C_1 z$  converges to  $y_{r_1}$  (on the left) and  $C_2 z$  converges to  $y_{r_2}$  (on the right). Any time  $y_{r_1}$ ,  $y_{r_2}$  or  $d$  change, there are small spikes in the graphs of  $C_1 z$  and  $C_2 z$  that are immediately reabsorbed. These spikes are due to the inertial approximation.

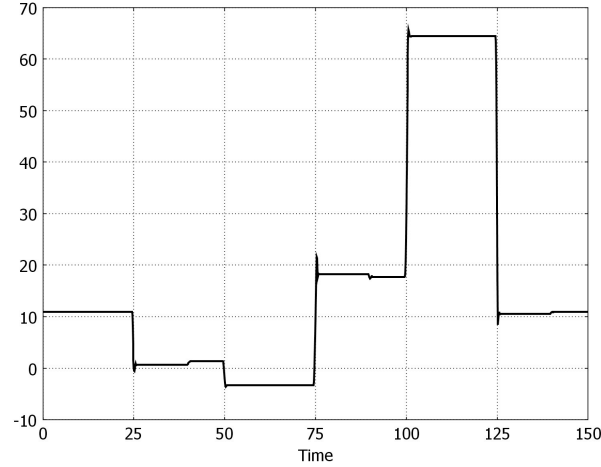


FIGURE 15.  $u_1(t) = \gamma_1(t)$  for  $0 \leq t \leq 150$ .

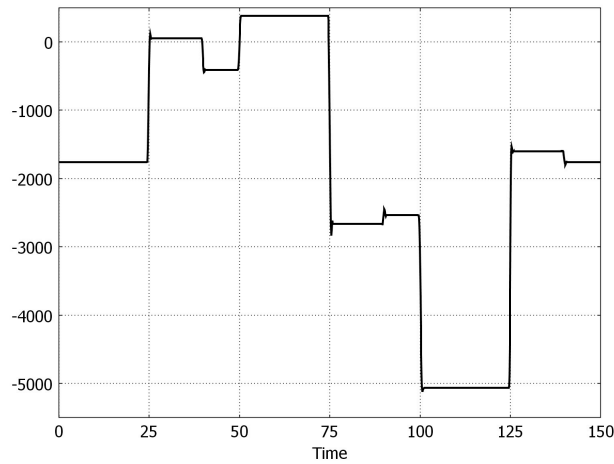


FIGURE 16.  $u_2(t) = \gamma_2(t)$  for  $0 \leq t \leq 150$ .

In Figure 15, we display the controller  $u_1(t) = \gamma_1(t)$  and in Figure 16, we display the controller  $u_2(t) = \gamma_2(t)$  for all time  $t$ . Near a time in which  $y_{r_1}$ ,  $y_{r_2}$  or  $d$  change, there is a short transient. After that, both graphs stabilize to a new value till a new change occurs.

In Figure 17 we have plotted the solution surface  $z(x, t)$  for  $0 \leq x \leq 1$  and  $0 \leq t \leq 150$ .

- (1) At  $x = 0$  (on the left side of the figure) we obtain the curve  $z(0, t)$  which approximates  $d(t)$  in (188).
- (2) At  $x = 0.25$  the solution  $z(0.25, t)$  quickly approximates  $y_{r_1}(t)$  in (189).
- (3) At  $x = 0.75$  the solution  $z(0.75, t)$  quickly approximates  $y_{r_2}(t)$  in (190).

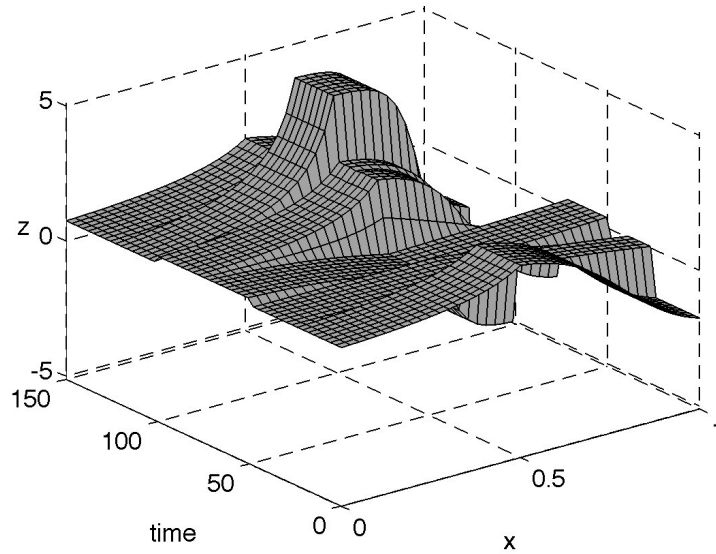


FIGURE 17. solution surface  $z(x, t)$  for  $0 \leq x \leq 1$  and  $0 \leq t \leq 150$ .

Finally, we are going to show an example where the disturbance and the signals to be tracked are all sinusoidal functions,

$$(192) \quad d(t) = 0.75 + 0.25 \sin\left(\frac{4\pi}{150}t\right),$$

$$(193) \quad y_{r_1}(t) = 1 + 0.25 \sin\left(\frac{2\pi}{150}t\right),$$

$$(194) \quad y_{r_2}(t) = 0.5 - 0.25 \sin\left(\frac{2\pi}{150}t\right),$$

for  $0 \leq t \leq 150$ . Here, the assumptions made on the structure of the exo-system (27) do not hold at any time, consequently, applying the above procedure does not produce signals  $C_1 z(t)$  and  $C_2 z(t)$  that converge to  $y_{r_1}(t)$  and  $y_{r_2}(t)$ , respectively. In order to isolate the magnitude of the errors  $e_i(t) = y_{r_i}(t) - C_i z(t)$  ( $i = 1, 2$ ) we chose as initial data for the state variable  $z$  the function  $\varphi(x) = Z(x)$ , so that the initial errors  $e_i(0)$  are identically zero. In Figure 18 we show the time evolution of both errors for the time interval  $0 \leq t \leq 150$ . As previously stated the error do not converge to zero, however their magnitudes remains small and the largest value is below  $2 \times 10^{-3}$ .

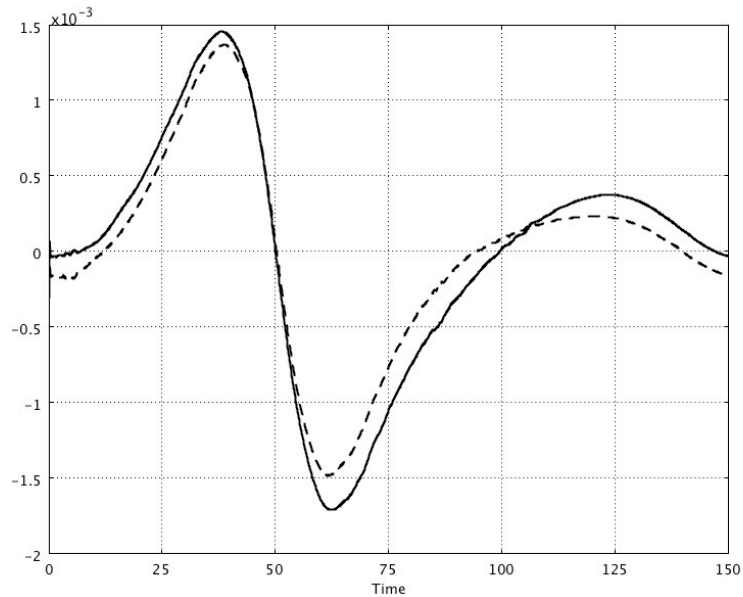


FIGURE 18. Errors  $e_1 = y_{r_1}(t) - C_1z(t)$  (solid line) and  $e_2 = y_{r_2}(t) - C_2z(t)$  (dashed line) for  $0 \leq t \leq 150$ .

### Acknowledgments

Eugenio Aulisa is supported in part by the National Science Foundation Grant NSF-DMS 0908177. David Gilliam is supported in part by the Air Force Office of Scientific Research under grant FA9550-12-1-0114.

### References

- [1] E. Aulisa and D.S. Gilliam, “Regulation of a controlled Burgers’ equation: Tracking and disturbance rejection for general time dependent signals”, Proceedings of American Control Conference, 2013, pp. 1290-1295.
- [2] A. Bensoussan, G. Da Prato, M.C. Delfour, S.K. Mitter, Representation and Control of Infinite Dimensional Systems, I, II,” Progress in Systems and Control, Birkhäuser, Boston 1992, 1993.
- [3] C.I. Byrnes, D.S. Gilliam, “Geometric theory of output regulation for nonlinear DPS,” *Proc. American Control Conference 2008*.
- [4] C.I. Byrnes, D.S. Gilliam, I.G. Laukó and V.I. Shubov, “Output regulation for linear distributed parameter systems,” *IEEE Transactions Automatic Control*, Volume 45, Number 12, December 2000, 2236-2252.
- [5] C.I. Byrnes and D.S. Gilliam, “Approximate Solutions of the Regulator Equations for Nonlinear DPS”, *Proc. IEEE Conference on Decision and Control 2007*.
- [6] C. I. Byrnes, D.S. Gilliam, V.I. Shubov, ”Geometric theory of output regulation for linear distributed parameter systems,” *Frontiers Appl. Math.*, (27) 139–167. SIAM, Philadelphia, PA, 2003.
- [7] Comsol 3.5a Multiphysics Modeling Guide, November 2008.
- [8] B.A. Francis, “The linear multivariable regulator problem,” *SIAM J. Control & Optimiz.* **15** (1977), 486-505.
- [9] I.M. Gel’fand and G.E. Shilov, “Generalized Functions, Vol 2: Spaces of Fundamental and Generalized Functions,” Academic Press 1968.
- [10] D. Henry, “Geometric Theory of Semilinear Parabolic Equations,” Springer-Verlag, 1989.
- [11] A. Isidori and C.I. Byrnes. Output regulation of nonlinear systems. *IEEE Trans. Autom. Contr.*, **AC-25**: 131–140, 1990.
- [12] A. Isidori, *Nonlinear Control Systems*, vol I, 3rd Edition Springer Verlag (New York, NY), 1995.

- [13] A. Isidori. *Nonlinear Control Systems*, volume II. Springer Verlag, New York, NY, 1999.
- [14] T. Kato, *Perturbation Theory of Linear Operators*, Springer-Verlag, 1966.
- [15] D. Salamon, Infinite-dimensional linear systems with unbounded control and observation: A functional analytic approach. *Trans. of American Math. Soc.*, v. 300, pp. 383-431, 1987.
- [16] M. Tucsnak and G. Weiss, *Observation and Control for Operator Semigroups*, Birkhäuser Advanced Texts / Basler Lehrbücher, 2009, XI, 483 p., Hardcover ISBN: 978-3-7643-8993-2.
- [17] T.I. Zelenyak, M.M. Lavrentiev Jr., M.P. Vishnevskii, *Qualitative Theory of Parabolic Equations, Part 1*, VSP, Utrecht, The Netherlands, 1997.

Department of Mathematics and Statistics, Texas Tech University, Lubbock, TX 79409-1042, USA

*E-mail*: [eugenio.aulisa@ttu.edu](mailto:eugenio.aulisa@ttu.edu) and [david.gilliam@ttu.edu](mailto:david.gilliam@ttu.edu)

*URL*: <http://www.math.ttu.edu/~eaulisa> and <http://www.math.ttu.edu/~dgilliam>